Joint Control During Arm Movements Performed in Reaching Activities of Daily Living

by

Dattaraj Sansgiri

A Thesis Presented in Partial Fulfillment
of the Requirements for the Degree
Master of Science

Approved March 2018 by the
Graduate Supervisory Committee:

Natalia Dounskaia, Co-Chair
Sydney Schaefer, Co-Chair
Christopher Buneo

ARIZONA STATE UNIVERSITY

May 2018

ABSTRACT

The ultimate goal of human movement control research is to understand how natural movements performed in daily reaching activities, are controlled. Natural movements require coordination of multiple degrees of freedom (DOF) of the arm. Patterns of arm joint control were studied during daily functional tasks, which were performed through the rotation of seven DOF in the arm. Analyzed movements which imitated the following 3 activities of daily living: moving an empty soda can from a table and placing it on a further position; placing the empty soda can from initial position at table to a position at shoulder level on a shelf; and placing the empty soda can from initial position at table to a position at eye level on a shelf. Kinematic and kinetic analyses were conducted for these three movements. The studied kinematic characteristics were: hand trajectory in the sagittal plane, displacements of the 7 DOF, and contribution of each DOF to hand velocity. The kinetic analysis involved computation of 3-dimensional vectors of muscle torque (MT), interaction torque (IT), gravity torque (GT), and net torque (NT) at the shoulder, elbow, and wrist. Using the relationship NT = MT + GT + IT, the role of active control and passive factors (gravitation and inter-segmental dynamics) in rotation of each joint by computing MT contribution (MTC) to NT was assessed. MTC was computed using the ratio of the signed MT projection on NT to NT magnitude. Despite a variety of joint movements available across the different tasks, 3 patterns of shoulder and elbow coordination prevailed in each movement: 1) active rotation of the shoulder and predominantly passive rotation of the elbow; 2) active rotation of the elbow and predominantly passive rotation of the shoulder; and 3) passive rotation of both joints. Analysis of wrist control suggested that MT mainly compensates for passive torque and provides adjustment of wrist motion according to requirements of each task. In

conclusion, it was observed that the 3 shoulder-elbow coordination patterns (during which at least one joint moved) passively represented joint control primitives, underlying the performance of well-learned arm movements, although these patterns may be less prevalent during non-habitual movements.

DEDICATION

I would like to dedicate this to my Mom, Dad, Sister and Grandmother. Without their love, support, and understanding I would not be half the man I am today.

ACKNOWLEDGMENTS

First and foremost, I would like to express my gratitude to my advisor, Dr. Natalia Dounskaia for providing me with an opportunity to work with her. Dr. Dounskaia, with her time and effort has thoroughly guided me in the concepts and fundamental role of control patterns in human bio-mechanics. She has taught me the importance of detailed evaluation of data by keeping an inquisitive mind-set which has molded me into an able researcher. Her emphasis on problem visualization with different perspectives and appropriating it into simple phases have helped me greatly in problem solving. Secondly, I would like to thank the rest of my thesis committee, Dr. Schaefer for teaching me importance in hypothesis testing and Dr. Buneo in the research ethics throughout my graduate studies. I would also like to thank all my co-researchers in the Motion Analysis Laboratory at Arizona State University for their support in thesis throughout my graduate studies. I would especially like to thank Dirk Marshall and Joshua Sarbolandi for their insights in my thesis . Finally, I'd like to thank my friends in USA and in India for their love and support especially during difficult times. I am greatly appreciative of Nikita Shanker for her invaluable support in the completion of my thesis.

TABLE OF CONTENTS

CHAPTER Page

LIST OF TABLES

LIST OF FIGURES

Chapter 1

INTRODUCTION

1.1 Problem Statement

Human joint movement is a complex closed-loop system of information transfer between the CNS and the limbs. Limbs are intricate structures of connected multi-joint segments. Movements involving in the rotation of these multiple joints involve a redundant number of degrees of freedom (DOF). When a movement-based decision is made, CNS sends appropriate control signals to the limb. These control signals generate necessary torques based on the limb movement. The ultimate goal of human movement control research is to understand how natural movements performed in daily activities work. Despite rapid advancement in neural control research, understanding the neural coordination in the manipulation of multiple degrees of freedom (DOF) of the arm is limited. Control parameters not only defines the movement of the arm from position A to position B in an optimum path without exceeding the joint constraints (Kinematics) but also the amount of torque required by the joints for that movement and the force to exert it to the surroundings. Understanding these control patterns can elucidate the concepts of neural movement coordination in the manipulation of multiple degrees of freedom (DOF).

Numerous research has been conducted on the interpretation and understanding of control patterns in two-dimensional and three-dimensional movement tasks. A research by Dounskaia and Wang (**Dounskaia and Wang**; **2014**), conducted task-based research on two - dimensional movement, where they determined the direc-

tion bias for redundant DOF in planar drawing tasks. Some of the task-based studies on three-dimensional movement are free-stroke drawing tasks for left diagonal and right diagonal in the para-sagittal plane (**Dounskaia and Wang**; **2015**), analysis of intersegmental dynamics during catching in typically developed children and children with development disorder (**Asmussen et al.**; **2014**), determination of kinematics of throwing arm during the penalty throw in water polo (**Feltner and Nelson**; **1996**), and many others. Despite all the research, joint control during daily functional tasks has not been studied.

Determining control patterns in daily activities, by breaking them down into a simple internal model of intersegmental joints and the CNS offers a unique perspective for interpreting the phase-wise categorization and changes in motor control caused by development, motor, learning, aging, and motor disorders. Deteriorations in neural control of movement are often associated with motion slowness – such as in the normal aging, Parkinson's disease, and stroke. Control Pattern studies can help in understanding the origins of slowness in weakened states of the CNS (**Dounskaia et al.**; **2009**).

1.2 Literature Review

1.2.1 Past Theories and Hypothesis

Learning complex tasks is usually perceived as a problem of mastering the multiple and redundant DOF of the system (**Caillou et al.**; **2002**). Redundancy refers to the presence of more number of DOF for a task than required, that is, same tasks can be performed using a different combination of joints (**Dounskaia**; **2014**). This

kinematic redundancy fascinated researchers starting from Bernstein (**Bernstein**; **1967**), who claimed that the main problem in a motor task mastering the multiple and redundant DOFs involved in it. Later, in 1999, Vereijken and Bongaardt (**Vereijken and Bongaardt**; **1999**) conducted an experiment which imitated ski-like movements in the frontal plane performing high amplitude, high-frequency side-by-side movements for a duration of 30 seconds over a 7-day span. This study tested the learning of motor task and the effects of phase dynamics on the learning. Their study proposed that a reduction in DOF redundancy is achieved by "freezing" the number of joints, reducing the complexity of the whole-body skill into a lower dimensional description of a coordinative structure of multi-linked joints. The second strategy suggested by Vereijken and Bongaardt (**Vereijken and Bongaardt**; **1999**) proposed the characterization of biological movements as the synchronization of various oscillators of the composing the motor system. These results suggested two strategies to reduce the high control parameters caused by DOF redundancy at the anatomical joints. First, freezing of joints to reduce the active DOF and second, the inclusion of rigid couplings between the joint, restricting the DOF to one. These studies provided an insight into the reduction of the complex variables introduced by DOF redundancy. Redundancy provides more flexibility in movement control and can be used by CNS for different purposes (**Latash**; **2012; Dounskaia**; **2014**). For example, an infinite number of joint angle trajectories can generate a specified hand path and speed by using different muscles (**Fraklin and Wolpert**; **2011**). Multiple theories pertaining to the control of human movements are proposed such as inverse dynamics approach, generalized motor program theory, equilibrium point hypothesis and optimal control approach in understanding the observed control patterns.

1.2.1.1 Inverse Dynamics Approach

Inverse dynamics approach suggests that during a movement, from the target position, CNS calculates the hand trajectory required for the particular task. From this trajectory, joint kinematics is determined and finally, joint torques are calculated which are provided as an input to the biomechanical model, the output for which generates the rotation of joint at the desired velocity (**Hollerbach JM**; **1982**)(Figure 1).

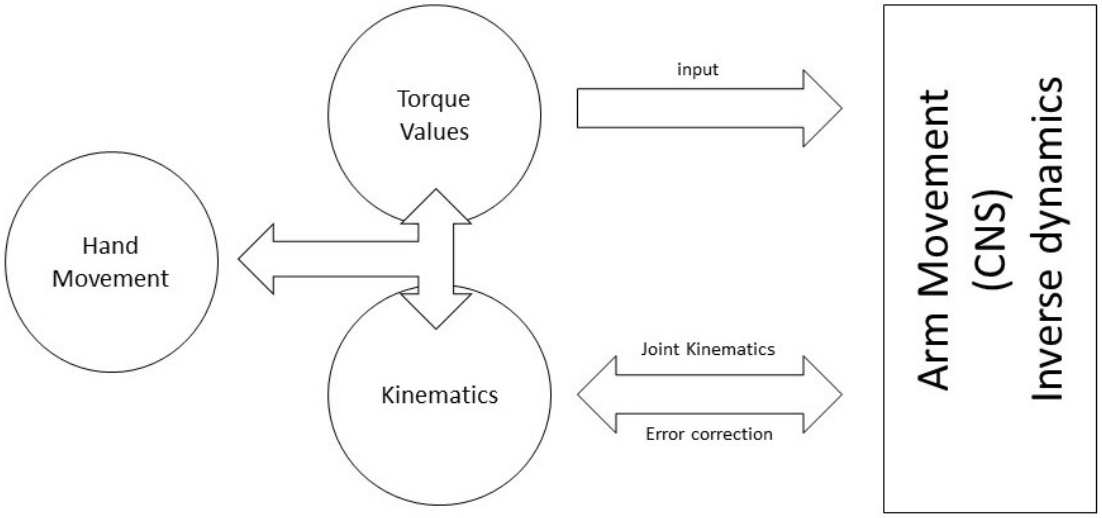

Figure 1: Visualization of Inverse Dynamics Approach

One major problem with this approach is the interpretation of bio mechanical model as a highly detailed one. The lack of a component capable of adapting to uncertainties of the model and adjusting to the unexpected changes makes this control inflexible (**Dounskaia**; **2010**).

1.2.1.2 Generalized Motor Program

The generalized motor program is a motor control theory developed by Schmidt (**Schmidt**; **1976a**). It suggests that the motor program for a class of actions is stored in memory resulting in a unique pattern of activity on program execution. Specific parameters must be supplied to the program which defines the execution of a particular trial as trial outputs can be altered by changes in the selected parameters. Although motor program also suggests that parameters can be modified to provide variations in the movement rate and amplitude, however flexibility of control is still limited to the original interpretation. That is, origin of each motor program is not clear (**Dounskaia**; **2010**).

1.2.1.3 Equilibrium Point Hypothesis (EP)

Equilibrium control hypothesis or Lambda model is based on a spring-like approximation of muscle properties (**Dounskaia**; **2010**). It suggests that the active movements can be the result of shifts in the equilibrium state of the motor system. It is considered by referring the following concepts: a) The length of the force invariant characteristics (IC) of the muscle together with the central and reflex systems sub serving its activity; b) tonic stretch reflex threshold (lambda); c) the equilibrium point defined in terms of lambda, IC and static load characteristics, which are associated with the notion that posture and movement is controlled by a single mechanism; and, d) the muscle activation area – the area of kinematic and command variables in which a rank order recruitment of motor unit tasks takes place (**Feldman**; **1986**). In essence, the trajectory for a movement is generated due to a gradual transition in

the equilibrium points where equilibrium point (Threshold control) is the state in which opposite muscles at a segment balance each other out. In this interpretation, motor neurons signals change the force-length characteristics of a muscle, hence shifting and maintaining the equilibrium of the total systems. While this theory displays promising results in single-joint movements, the simplicity disappears when analyzing complete multi-joint movements.

1.2.1.4 Optimal control approach

Optimal control approach works in the optimization of a cost function such as muscle energy expenditure, movement time, accuracy, smoothness, and others (**Todorov**; **2004**). It uses cost function reduction for the variables dependent on the movement task. For example, reducing the cost function of the position and trajectory control can act as a task-variable for reaching movements. As multiple task factors are responsible, complications such as output being the weighted sum of all the task factors or effectively deciphering the performance of motor tasks can be difficult.

1.2.1.5 Uncontrolled Manifold Hypothesis (UCM)

In UCM, it is theorized that CNS does not eliminate DOF redundancy, ensuring a flexible and stable performance of motor tasks. In a system where CNS has the choice (synergies) of selecting different combinations of joint DOF for the same spatial movement of hand, stabilization offered by these choices at joint level can be assessed by the stabilization of hand trajectory. The idea is to use

joint space as the embedding space to measure the variance of all choices (**Schöner**; **1995; Scholz and Schöner**; **1999; Latash et al.**; **2007**). The hypothesis is then, at any given point during the movement, joint configurations vary primarily within their subset rather than outside of it. Due to the consideration of the variation of all the synergies in a spatial plane, problems similar to optimum control could be seen. Also, more the repetition of the tasks, better is the accuracy, making it more difficult for analysis.

1.2.1.6 Leading joint hypothesis (LJH)

This thesis is based on leading joint hypothesis (LJH) (**Dounskaia** ; **2005**; **2010**), which provides an alternative interpretation to the human movement control system. According to the hypothesis, an organizational principle is necessary to perform a task in a single motion. This organizational principle is based on the ability of the CNS to make a selection and provide a control signal to the leading joint (selected in the most efficient way for the task) which rotates the leading joint accordingly. The CNS takes advantage of the passive factors acting at the joins, including gravity and multi-link structure of the human arm to cause a motion-dependent mechanical interaction which rotates other linked joints (Figure 2). This motion-dependent mechanical interaction is termed as 'Interaction Torque' (IT).

To test this hypothesis, the control pattern for three reaching movements (forward, shoulder level, and eye level reaching) is developed. The table below shows the expected control pattern for the reaching movement.

Table 1, shows the predicted control for the reaching tasks. As reaching tasks are in the sagittal plane, flexion/extension DOF are hypothesized to be predominant.

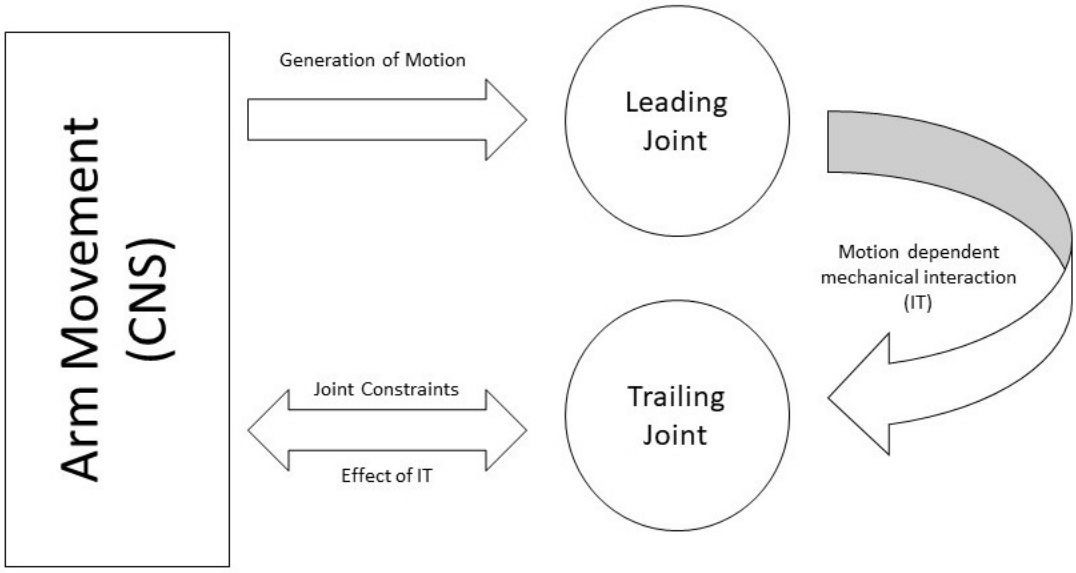

Figure 2: Visualization of Leading Joint Hypothesis

For a reaching task, shoulder joint must rotate first to adjust the trajectory and then elbow extends to reach the final position.

Table 1: Expected Result

Reaching Movement	Phase 1	Phase 2
Leading Joint DOF	Shoulder Flexion	Elbow Extension
Trailing Joint	Elbow (Passive)	Shoulder (Passive)

1.3 Anatomy and Mechanics

In this section, in-depth concepts of the human multi-link joint such as the structural and functional classification, joint axial DOF and mechanical constraints are described. The types of joints in the human body are classified either according to the structure of the joint or the function of the joint. Here, only the functional signif-

icance of the joint is considered based on the importance of the movement permitted at each joint (joint constraints) in the research study parameters as shown in Figure 3.

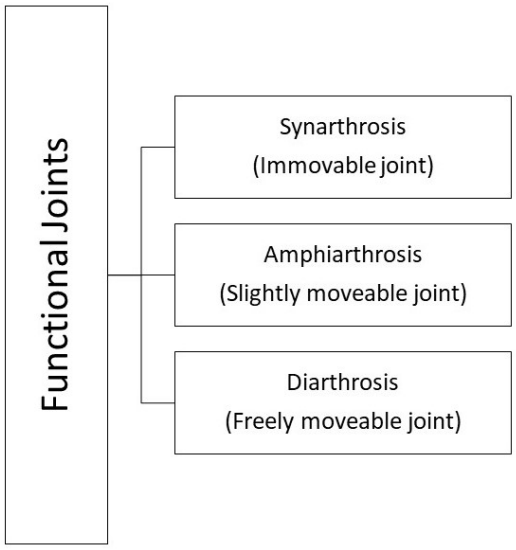

Figure 3: Types of Joints

Among these functional joints, the joint considered in this study is the Diarthrosis type of joint.

Diarthrosis Joint – These types of joint are capable of movements in one or more planes. The availability of movement in these planes is called DOF, and the number of planes or axes along which the joint rotates is equal to the number of DOFs available for the joint. These joints are lubricated by the synovial fluid, secreted by a ligamentous tissue called joint capsule. Additional ligaments which are not connected to the joint capsule provide stability to the joint. Diarthrosis joints are further classified based on their role and axes of rotation they provide. Classifications related to this study for shoulder, elbow, and wrist are given below.

1.3.1 Anatomy and Mechanics of Shoulder Joint

The shoulder joint is an Enarthrodial joint, which a type of Diarthrodial joint known for its spheroidal shape. It is a true ball and socket joint having the rotational capability in all three planes as shown in the Figure 4 below.

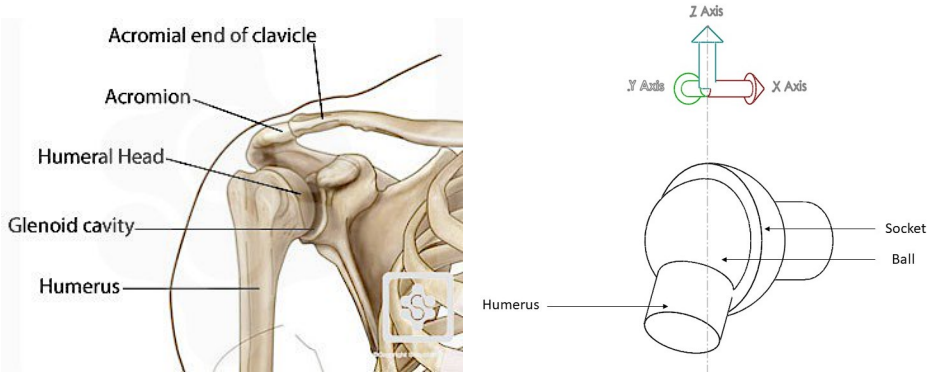

(a) Shoulder Joint (b) Ball and Socket

Figure 4: Shoulder Anatomy and Joint Configuration

Source 4(a):https://www.shoulderdoc.co.uk/article/1177

Being a spheroidal joint, shoulder joint exhibits three DOF in the sagittal, frontal, and transverse plane. Rotation along the X-axis in the sagittal plane is for shoulder flexion/Extension DOF. Similarly, rotation along the Y-axis in the frontal plane is for the abduction/adduction DOF, and the rotation along the Z-axis in the transverse or axial plane is for the internal/external rotation. A combination of three DOFs enables rotation of the arm in 3D space.

1.3.2 Anatomy and Mechanics of Elbow Joint

Elbow joint consists of two components which specify their DOF, the first one is a Ginglymus or hinge joint at the elbow which allows a wide range of movement but only in one plane and the second joint is Trochoidal or pivot joint which provides rotation in one plane. Figure 5 below shows the anatomical and mechanical configuration of the elbow joint. The hinge joint provides the elbow with flexion/extension DOF and pivot joint provides elbow with pronation/supination movement.

1.3.3 Anatomy and Mechanics of Wrist Joint

The wrist joint is a Biaxial joint of the Diarthrodial joint category. This joint is biaxial in nature, that is, it enables the rotation of wrist in two planes (Axial plane and frontal plane). The figure below shows the biaxial joints present in the wrist joint. Rotation about X-axis enables the rotation about the sagittal plane which is radial/ulnar deviation and rotation about Y-axis enables rotation about frontal plane which is flexion/extension. Wrist joint configuration can be seen in Figure 6.

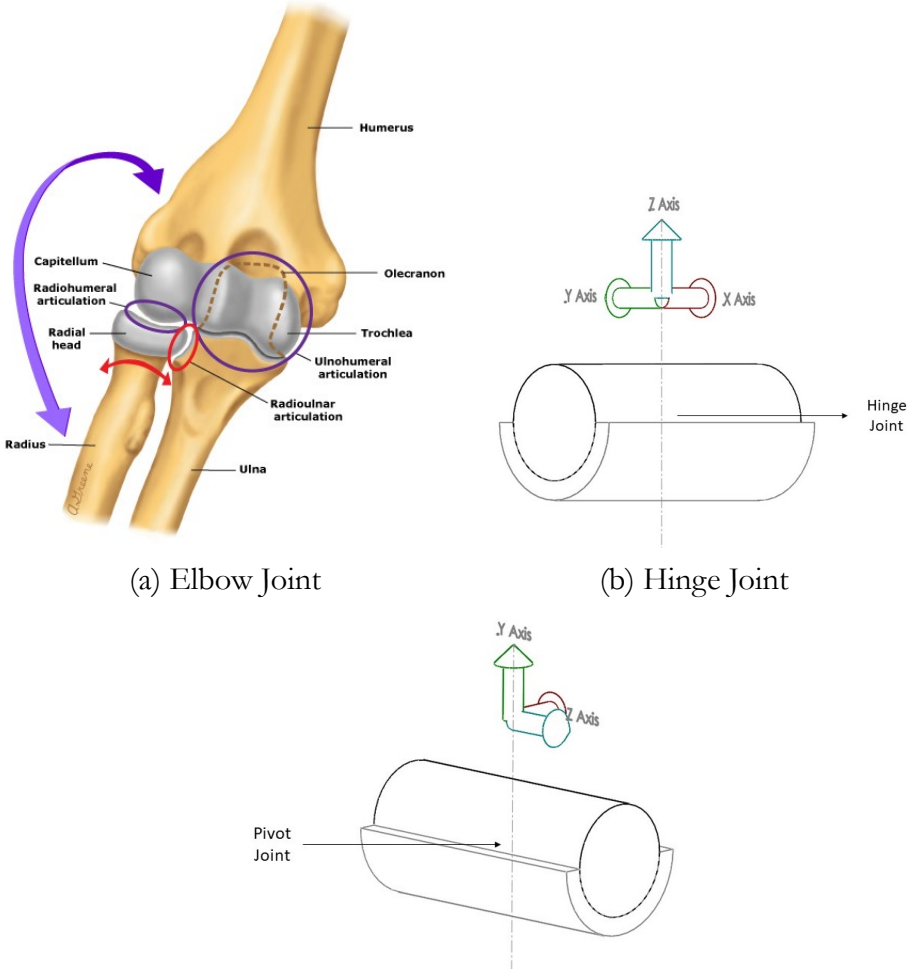

(a) Elbow Joint (b) Hinge Joint

(c) Pivot Joint

Figure 5: Elbow Anatomy and Joint Configuration

Source 5(a):https://s0www.utdlab.com/contents/image?imageKey=EM%2F66874

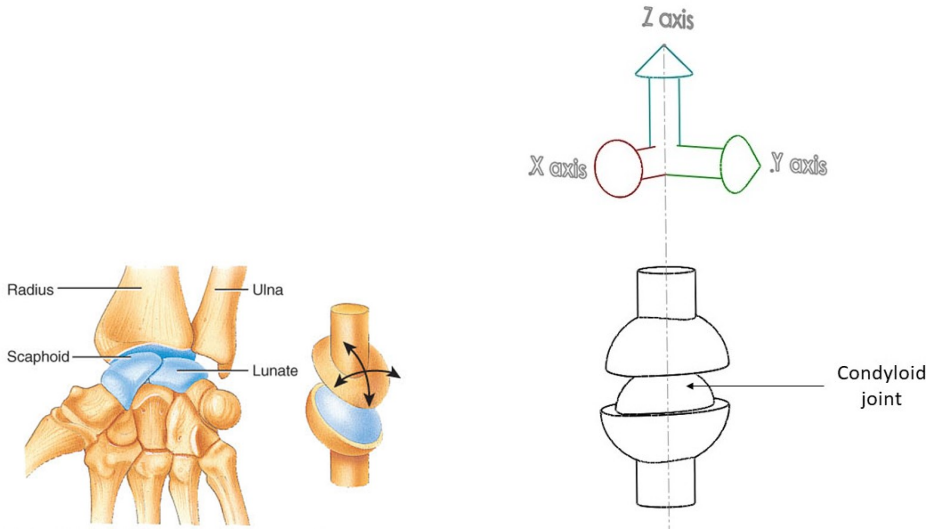

(a) Condyloid Joint (b) Biaxial Joint

Figure 6: Wrist Anatomy and Joint Configuration

Source 6(a):https://sites.google.com/site/jointproject435/wrist/wrist-movements

Chapter 2

METHODS

2.1 Experimental Design

This section describes the development of the experimental design, equipment used for analysis, and declaration of the joint coordinate system for kinematic and kinetic study.

2.1.1 Participants

14 young adults (7 males and 7 females, 21.7 $\pm$ 2.2 years of age), graduates and undergraduates, were selected from Arizona State University for conducting experimental procedures. Each participant received either a class credit or $10 for their participation in the research study. A questionnaire was prepared to determine the participant's dominant hand, which was adapted from the questionnaire of Edinburgh Handedness Inventory (**Oldfield**; **R.C.**; **1971**). Only right-handed participants were included in the study as all the procedures were performed on the right arm. Participants were also asked to complete the patient assessment and self-evaluation sections of the American Shoulder and Elbow Surgeons Standardized Shoulder Assessment Forms (ASES) to test for any symptoms of shoulder injury (**Richards**; **Robin R**; **et al.**; **1994**). Further, demographic information and informed consent was also received from each participant before their participation in the study. Arm length and length of upper arm, forearm and hand segments

were measured along with participant's height and weight. Active range of motion (ROM) were taken using a goniometer for shoulder (flexion/extension, abduction/adduction and internal/external rotation), elbow (flexion and resting flexion) and wrist (flexion/extension and radial/ulnar deviation). Each participant's blood pressure was measured but not disclosed to them prior to completion of the procedures/tests ensuring unaltered / unaffected performance.

2.1.2 Motion Capture and Marker Locations

Eight Kestrel motion capture cameras (Motion Analysis Corporation, Santa Rosa, CA) were placed around the lab area, facing towards the center of the lab. Before each subject's test session, all cameras were calibrated, and setup files were saved as per the reference manual. Thirteen 1 cm diameter retro-reflective pearl markers were placed on the subject at the specified points (see Figure 7) on the trunk along the right arm. The thirteen points used, which were same for all the tests, were: second metacarpophalangeal joint, fifth metacarpophalangeal joint, radial styloid, ulnar styloid, forearm, medial epicondyle, lateral epicondyle, head of the biceps brachii, right clavicle, right acromion, left acromion, seventh cervical vertebra, and xiphoid process. The index marker was not used in this experiment.

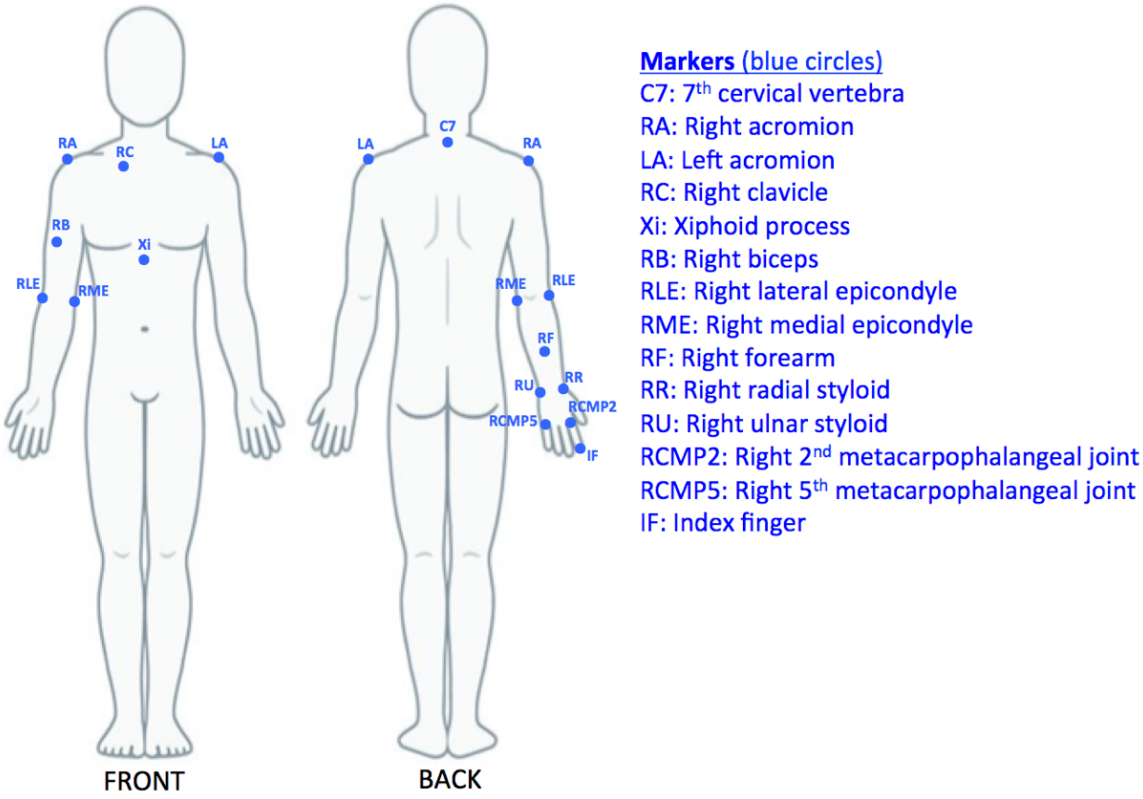

Figure 7: Placement of Markers

Recordings of the marker, development of rigid-body figure and post-processing of data were executed using Cortex Version 6.0 software (Motion Analysis Corporation, Santa Rosa, CA). Each movement was recorded at 200 Hz sampling frequency and timed using a metronome. Data post-processing included handling missing data, dropped markers in the complete trial and saving the 3D coordinates and time frame for all the markers. Cubic splines were used as an alternative for markers in the missing data sets.

2.1.3 3D Reaching Tasks

Participants were asked to perform three 3D functional movement tasks that represented activities of daily living (ADLs : Forward reaching, shoulder level reaching and eye level reaching). These tasks were performed in a seated position, on a chair at a table placed at the central location in the room where all the markers were visible to the cameras. Participants were strapped to the chair with the strap over the left shoulder and going diagonally across the body to prevent trunk movement and avoid the inclusion of redundant DOF during the movement. In the initial position, the hand was placed on the table in such a manner so that the wrist was at the edge of the table, the upper arm was vertical, and the lower arm was horizontal as shown in Figure 8. The target position for reaching was individualized for each participant using 80% of the length of the participant's forearm (lateral epicondyle to ulnar styloid). During forward reach, participants moved an empty soda can in a straight motion (away from the shoulder) and placed it on the table at a distance equal to 80% of the forearm length. During the reaching tasks at the shoulder and eye level, a shelf of the corresponding height was positioned at the horizontal distance of 80% of the

forearm length from the initial position, and participants placed the can on the shelf in front of the right shoulder or eye. Each task was performed three times in each condition, with rest in between each trail as needed.

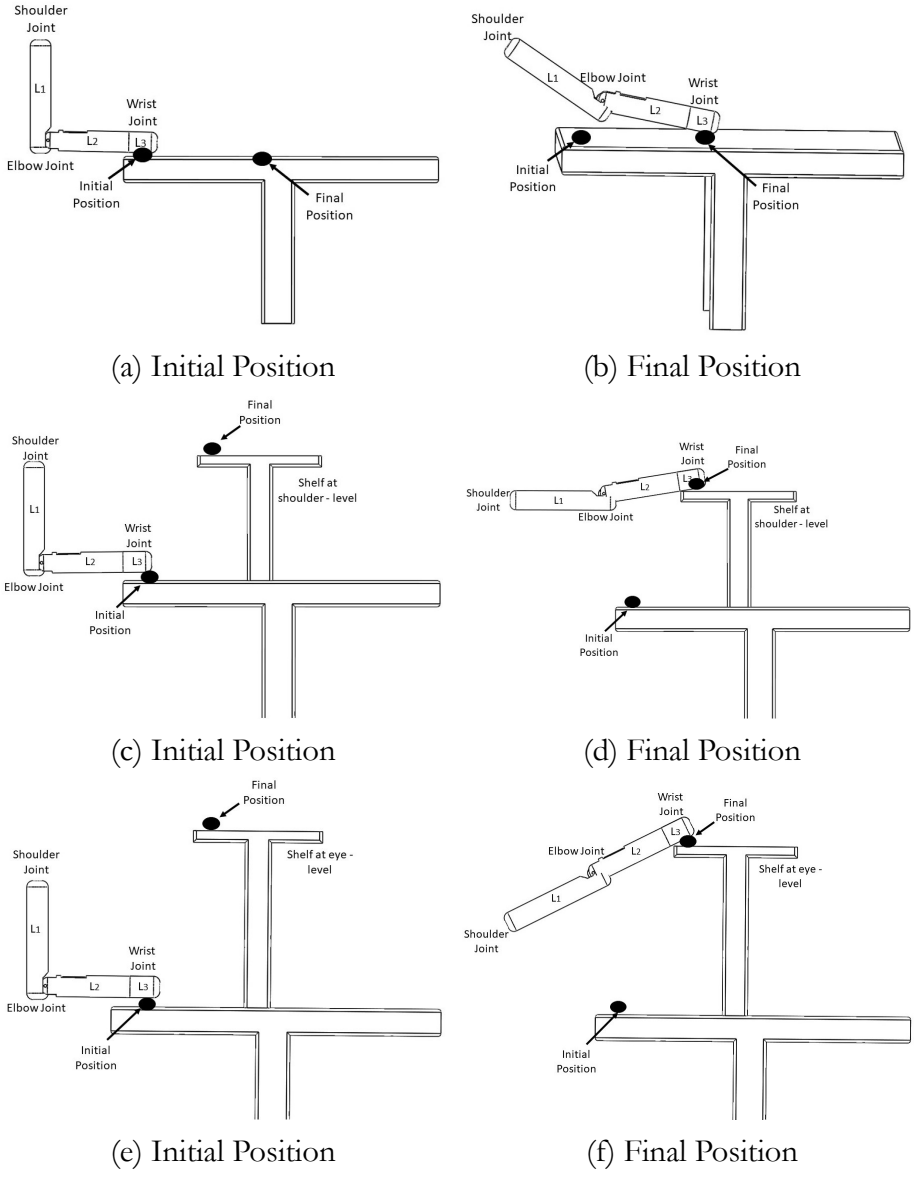

(a) Initial Position (b) Final Position

(c) Initial Position (d) Final Position

(e) Initial Position (f) Final Position

Figure 8: 3D Tasks

2.2 Global and Local Coordinate system

Global coordinate system (GCS) was defined by the Cortex at the intersection of all the cameras. Xg, Yg and Zg in the Figure 9 shows the GCS defined.

2.2.1 Segment coordinate system

Segment coordinate system was defined at the immovable trunk, upper arm, forearm and hand (**Hirashima et al.**; **2006**) (Figure 9). The trunk coordinate system was defined as (x0, y0, z0) where x0 is a unit vector pointing from the midpoint of markers at RC and C7 to the marker at LA, z0 is a unit vector pointing upwards and y0 unit vector is the cross product of the above two vectors x0 and z0. Similarly, segment coordinate system at the upper arm was defined as (x1, y1, z1), forearm as (x2, y2, z2) and hand coordinate system as (x3, y3, z3). Segment coordinate systems were defined by its distance from the GCS and orientation of the axes were calculated using direction cosines. A rotation matrix was developed consisting the values of the cosine of the angle made by segment coordinate system to the GCS.

$$R_i = [x'_i \quad y'_i \quad z'_i] \tag{2.1}$$

where,

i = DOF from shoulder to wrist, (0 = Trunk, 1 = Shoulder, 2 = Elbow and 3 = Wrist)

R = Rotation Matrix at i^{th} DOF,

x'_i = the direction cosines of i^{th} LCS to the X - axis of GCS,

y'_i = the direction cosines of i^{th} LCS to the Y - axis of GCS, and

z_i' = the direction cosines of i^{th} LCS to the Z - axis of GCS,

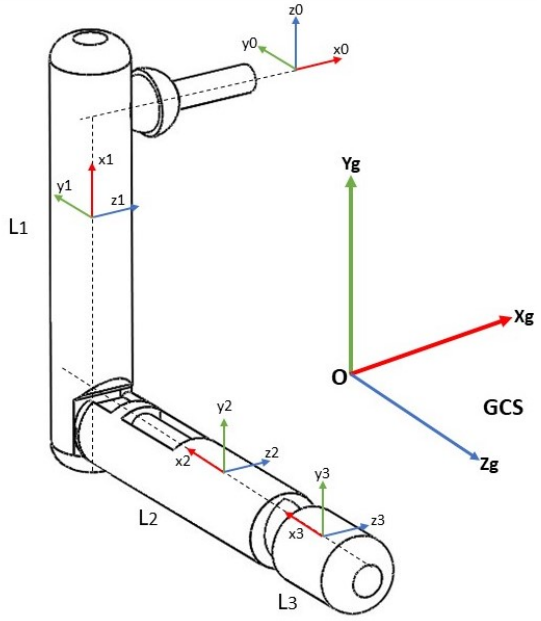

Figure 9: Global (GCS) and Segment Coordinate System

This coordinate system was developed for the calculation of angular velocity and inertia tensor which is discussed later in Kinematics section

2.2.2 Joint coordinate system

The Joint coordinate system was defined at each joint: shoulder, elbow, and wrist. The joint coordinate system was used for the calculation of torques (Discussed later). The DOF rotations along these axes define the acceleration of joints, and in-turn the torques at these joints. Initially, unit vector k1 was defined along the segment, so, k1 was a vector pointing from elbow to shoulder and considered at shoulder. Similarly, vector k2 was defined along forearm pointing towards the shoulder, taken at the

elbow and vector k3 was defined along the length of the hand pointing towards the elbow and taken at the wrist. Similarly, vector j1 was calculated by taking the cross product of vector k1 with axis z0 of segment coordinate system and vector i1 was calculated by taking the cross product of vector k1 and j1, forming a joint coordinate system at the shoulder. Similarly, joint coordinate systems at elbow and hand were defined as shown in the Figure 10.

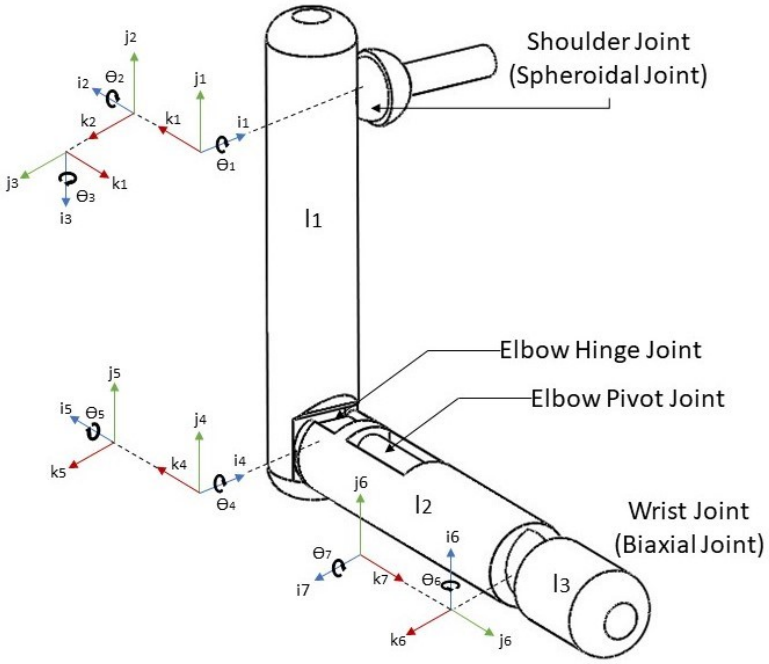

Figure 10: Joint Coordinate System

2.3 Kinematics and Kinetics

After post-processing of the data in Cortex, time and coordinate data for each marker were saved in a TRC file. This marker position data was passed through a second-order zero-lag low pass 7 Hz Butterworth filter to make the frequency

response as flat as possible, and then a zero phase forward and a backward filter was applied to reduce phase lags. Parameters such as the mass of each segment, longitudinal center of mass (CM) position and distance of CM from all the axial locations were adopted from the adjustments to inertia parameters by Paolo de Leva (**De Leva**; **1996**) to the initial studies by Zatsiorsky-seluyanov (**Zatsiorsky-seluyanov**; **1990**; **1993 and 1983**).

2.3.1 Kinematics

Kinematics describes the position and orientation of human arm in 3D. This section outlines the methods used in understanding kinematic data such as posture and orientation of the local coordinate system, DOF excursion and the contribution of each DOF to hand velocity.

2.3.1.1 Hand Trajectory in Sagittal Plane

Trajectory of the end-point (Hand) is characterized by a number of consistent kinematic characteristics observed during various direction, amplitude, speed and load conditions (**Dounskaia**; **2007**). Analysis of hand trajectory profile helps to examine the disturbances traced by hand the from initial position to final position. For tracing hand trajectory in the sagittal plane, midpoint of the marker at RR and RU refer (Figure 11) was taken and traced across Y-Z plane (Sagittal plane).

2.3.1.2 Segment and Joint Velocity

Segment velocity (ω_i) is first calculated for each segment and then joint angular velocity ($\dot{\theta}_i$) is derived from segment velocities. A rotating object in 3D space has one rotational axis at each movement, and its rotatory motion can be expressed using the angular velocity vector (**Hirashima et al.**; **2006**; **supplementary text**). The magnitude of this vector represents angular velocity, and its direction represents the rotational axis at which it rotates. Segment angular velocity was calculated using the below equation used by Feltner and Nelson (**Feltner and Nelson**; **1996**).

$$\omega_i = [\frac{d(y_i)}{dt} \cdot z_i] * x_i + [\frac{d(z_i)}{dt} \cdot x_i] * y_i + [\frac{d(x_i)}{dt} \cdot y_i] * z_i \tag{2.2}$$

(i = 0: trunk, 1: Upper arm, 2: Forearm, 3: Hand)

Joint angular velocity was calculated as the angular velocity of the segment relative to its proximal segment as follows (**Hirashima et al.**; **2006**).

$$\dot{\theta}_i = \omega_i - \omega_{i-1} \tag{2.3}$$

(i = 1: Shoulder, 2: Elbow, 3: Wrist)

$$\dot{\theta}_i = \sum_{r=1}^{n} \dot{\theta_{i-r}} \tag{2.4}$$

where,

r = 1,…,n (Number of DOF at that joint)

2.3.1.3 DOF dispalcements

DOF displacements can be defined as the rotation of each DOF along their axis of rotation. Calculation of DOF displacement helps in visualizing the extent of rotation of each DOF. After the calculation of joint angular velocities, DOF displacements are calculated by integrating the values of joint angular velocities at each DOF with respect to time. Counter-clockwise rotation across the axis of rotation is considered positive rotation and clockwise rotation is considered as negative rotation. The following Table 4shows positive and negative DOF rotations for the respective 7 DOF of arm:

Table 2: DOF displacements

Joint	+ve DOF Rotation	-ve DOF Rotation
Shoulder	Flexion	Extension
	Abduction	Adduction
	Internal Rotation	External Rotation
Elbow	Flexion	Extension
	Pronation	Supination
Wrist	Flexion	Extension
	Radial Deviation	Ulnar Deviation

Table 4 shows the 7 DOF considered at the joints and their axial rotation. Rotation about their axis brings about rotation of the joint along that DOF.

2.3.1.4 Contribution of DOF to Hand Velocity

It was necessary to assess how much each DOF contributed to the total hand velocity during the categorized phases. Initially, hand translational velocity was calculated by differentiating the marker values of the midpoint of Radius (RR) and Ulnar

marker (RU) with respect to the frequency of the time period for each trail. Then, DOF velocity contribution values were calculated by employing the equation used by Dounskaia and Wang (**Dounskaia and Wang**; **2014**).

$$|v| = \sum_{i=1}^{7} (v_i \cdot v_u) \ m/s, \tag{2.5}$$

where v_u is the unit vector of the hand translational velocity and v_i is the vector of the translational velocity of the hand produced by the rotation at i_{th} DOF (**Feltner and Nelson**; **1996; Hirashima and Ohtsuki**; **2008**). v_i is calculated as,

$$v_i = \ w_i \times p_i \tag{2.6}$$

where, w_i is the angular velocity at i_{th} DOF and p_i is the vector from the joint center to the hand. Hand velocity is represented by v_i on the unit vector v_u.

2.3.1.5 Joint and Segment Angular Accelerations

For calculating torques, it is essential to determine the segment and joint angular accelerations which are used in the equations of motion (described later). Joint angular acceleration at each DOF was calculated as the dot product of the derivative of joint angular velocity with respect to time and the unit vectors defining the joint coordinate system (**Hirashima et al.**; **(2007)**). For example, joint angular acceleration at shoulder for first anatomical DOF derived from Hirashima et al., can be calculated as:

$$\ddot{\theta}_i = \frac{d(\dot{\theta}_{i-r1})}{dt} * i1 \tag{2.7}$$

here,

r1 = Shoulder DOF for flexion/extension,

i = 1: Shoulder, 2: Elbow, 3: Wrist).

$\ddot{\theta}_i$ is substituted in the equation of motion for obtaining the torques. The relation between segment angular acceleration and joint angular acceleration can be expressed as follows (**Hirashima et al. 2006; Craig**; **1989 (Section 6.2)**)

$$\dot{\omega}_i = \dot{\omega}_{i-1} + \ddot{\theta}_i + \Omega_i \times \dot{\theta}_i \tag{2.8}$$

where,

Ω_i = angular velocity vector of each joint coordinate system (Like Equation 1), and

i = 1: Shoulder, 2: Elbow, 3: Wrist.

2.3.2 Kinetics

Kinetic behavior of a human arm can be described as the rate of change in arm configuration with relation to the joint torques exerted by the joints in human arm (**Harry Asada**; **2005**). This relation can be expressed using a set of differential equations called equation of motion. Kinetics provides information on the amount of force/torques required by the manipulator, in this case, human hand, to rotate its joints in 3D space and to interact with its surrounding. The current understanding of different torques in the rotation of each joint is based on the basic principle of classical mechanics that the motion at each joint is determined by net torque (NT) which is the sum of muscle torque (MT) and the passive torque acting at a joint which is the sum of gravitational torque (GT) and interaction torque (IT) caused by mechanical interactions of the limb segments. MT is generated by the muscle activity

and elasticity of passive tissues surrounding the joint (**Dounskaia and Shimansky**; **2016**).

2.3.2.1 Calculation of Torques

The Newton-Euler formulation is used to calculate the torques at each segment (**Hirashima et al.; Craig**; **1989**). The Newton-Euler formulation is derived from the direct interpretation of Newton's second law of motion, which describes dynamic systems in terms of force and momentum. This equation encompasses all the forces and moments acting on individual segments, and include the constraint forces which act between each link (**Harry Asada**; **2005**). The motion of a rigid body can be decomposed into translational motion and rotational motion. Translational motion is the motion of the body w.r.t a point fixed anywhere on the rigid body, while the latter is the rotational motion of the body across a selected point. The former that is the translation of body with respect to the coordinate system at an arbitrary point is described as Newton's equation of motion for the mass particle, while rotational motion calculation is referred to as Euler's equation of motion. The free body (Figure 11) shows all the forces and moments acting on the i^{th} segment. Let v_{ci} be the linear velocity of the segment i with respect to the global coordinate system. The inertial force is given by $-m_i\dot{v}_{ci}$, where m_i is the mass of the segment and $\dot{v}_{ci}$ is the derivative of v_{ci}. So, the equation of motion is obtained by adding the inertial force to the static balance of forces (**Harry Asada**; **2005**). In static holding, the only force acting on the segment is the gravitational force. Hence, the balance of linear forces are given by,

$$f_{i-1,i} - f_{i,i+1} + m_i g - m_i \dot{v}_{ci} = 0, \tag{2.9}$$

i =1,…, n

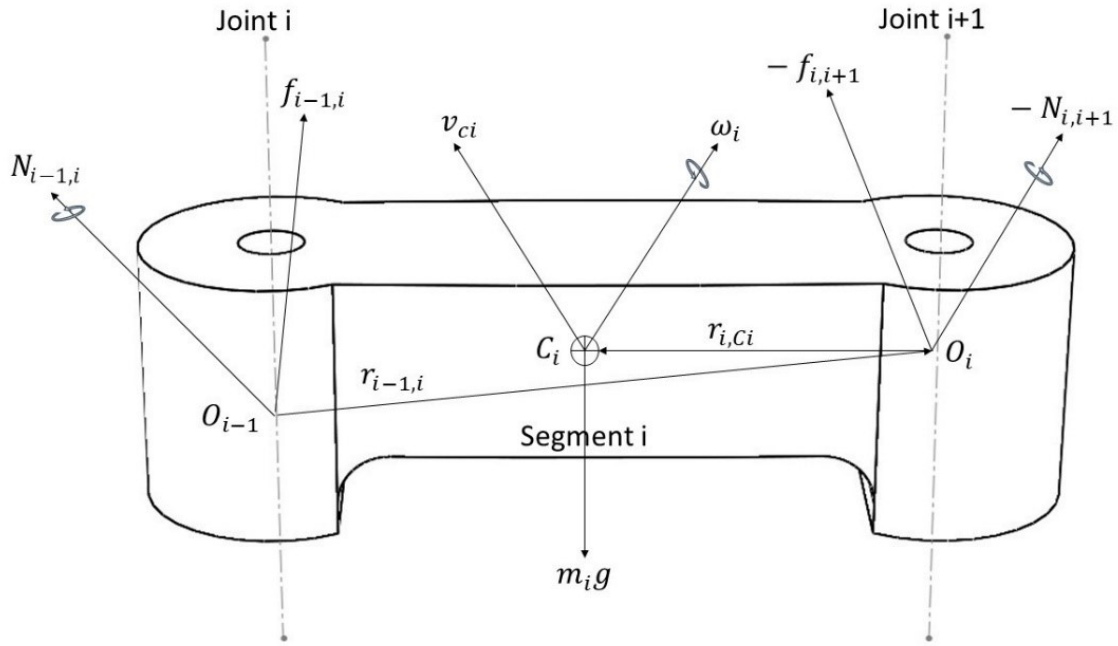

Figure 11: Free body diagram (Translation and Rotation at Joint i)

As mentioned earlier, the rotational motion is described by Euler's equation of motion. Similarly, the inertial tensor was calculated by adding inertial torques to the static moments for dynamic equations. So, the inertial tensor (I_i) of each segment with respect to a coordinate system that has its origin at the center of mass of the segment is oriented the same as the GCS (**Hirashima et al.**; **2006**), and is calculated by the formula derived from Hirashima's article as follows:

$$I_i = R_i * I_i' * R_i' \tag{2.10}$$

where,

R_i is derived from equation 1,

$$I_i' = \begin{bmatrix} I_{xi} & 0 & 0 \\ 0 & I_{yi} & 0 \\ 0 & 0 & I_{zi} \end{bmatrix},$$

$I_{xi} = m_i * (kx_i * l_i)^2, I_{yi} = m_i * (ky_i * l_i)^2, I_{zi} = m_i * (kz_i * l_i)^2,$

m_i is the mass of the segment (derived from De Leva's, article),

l_i = length of the segment, and

$kx_i,\ ky_i,\ kz_i$ = Parameters of the radius of gyration.

Finally, from Newton's second law, the inertial torque acting on the segment I is given by the rate of change of the angular momentum of the segment in that instant. So, adding all the terms, including the gyroscopic torque in similar rendition of equation (2) for joint coordinate system, the balance of moments yields,

$$N_{i-1,i} - N_{i,i+1} - (r_{i-1,i} + r_{i,Ci}) \times f_{i-1,i} + (-r_{i,Ci}) \times \left(-f_{i,i+1}\right) - I_i\dot{\omega}_i - \omega_i \times (I_i\omega_i) = 0 \tag{2.11}$$

i = 0: trunk, 1: Shoulder, 2: Elbow,3: Wrist

For the calculation of torques across non-orthogonal axes, equations derived by Hirashima et al., (**Hirashima et al.**; **2006**) were used for the calculation of the torque at each segment joints. NT, GT and IT for the joints at shoulder, elbow, and wrist were computed. MT was computed as the difference MT = NT - (GT + IT). NT is the resultant torque generated at i^{th} joint, MT provides torque by the muscles for rotation, GT is the torque due to the downward action of gravity, and IT is the torque due to inter-segmental linking of the joints. For better visualization of torque vectors, scalar projections of MT, GT and IT on NT were used and graphed.

2.4 Muscle Torque Contribution

Distinguishing the active and passive torque components at each joint provides insight into the organization of control of each joint and the entire movement (**Gribble and Ostry**; **1999; Hoy and Zernicke**; **1985; Koshland et al.**; **2000; Pigeon et al.**; **2003; Putnam**; **1993; Sainburg et al.**; **1993**; **1999; Sainburg and Kalakanis**; **2000; Schneider et al.**; **1990; Virji-Babul and Cooke**; **1995; Zernicke and Schneider**; **1993**). Muscle torque contribution (MTC) is the ratio of signed MT projections on NT to the magnitude of NT at each joint. Equation (**Dounskaia and Shimansky**; **2016**) was used to calculate MTC.

$$MTC \; = \; \frac{1}{n} \sum_{i \, = \, 0}^{n} f\left(i\right), \tag{2.12}$$

where,

Table 3: DOF displacements

$$f\left(i\right) = \begin{array}{cc} MT_NT/NT & \text{if } 0 < MT_NT < \text{NT}, \\ 1 & \text{if } MT_NT \geq \text{NT}, \\ 0 & \text{if } MT_NT < 0 \end{array}$$

Here, MT_{NT} is MT projection on NT, n is the total number of data points within a movement trial; $i = 1, 2, n$ is the number of iterations for the summation of values. Methods for the calculation of MTC were adopted from the studies of horizontal movements performed in (**Dounskaia et al.**; **2002a; Lee et al.**; **2007**) and 3D movements Dounskaia and Wang, 2014.

The purpose of calculating MTC was to determine the role of MT in rotating the particular joint for the movement trials. MTC values close to 0 at a joint sug-

gested that the joint moved passively due to the action of the sum of GT and IT, and values close to 1 indicated that the joint moved actively, because of MT. Phases were developed by studying the switching of the control from positive to negative movement.

Chapter 3

RESULTS

3.1 Forward Reaching Movement

3.1.1 Hand Trajectory in the Sagittal Plane

During arm movements, the trajectory of the end point (Hand) is characterized by a number of consistent kinematic characteristics observed during various direction, amplitude, speed, and load conditions (Dounskaia, 2007).

Trajectory of the hand was considered for observing the discrepancies or jitters in the movement which might cause changes in the hand velocity. Due to the movement predominantly being restricted in the sagittal plane, Y-Z axis of the markers on hand were considered with respect to the global coordinate system. Figure 12 displays a representative hand trajectory where a displacement of 0.2 m in the horizontal axis and an elevation of 0.05 m in the vertical axis is observed for the execution of movement. The smooth movement suggests that the goal is reached due to a continuous velocity change and that there are no interruptions in the hand velocity. The markings on the trajectory indicate the change in phases. The classification of phases is done by the change in the control patterns exhibited by the shoulder and elbow joint for a movement. More information of phases is discussed later.

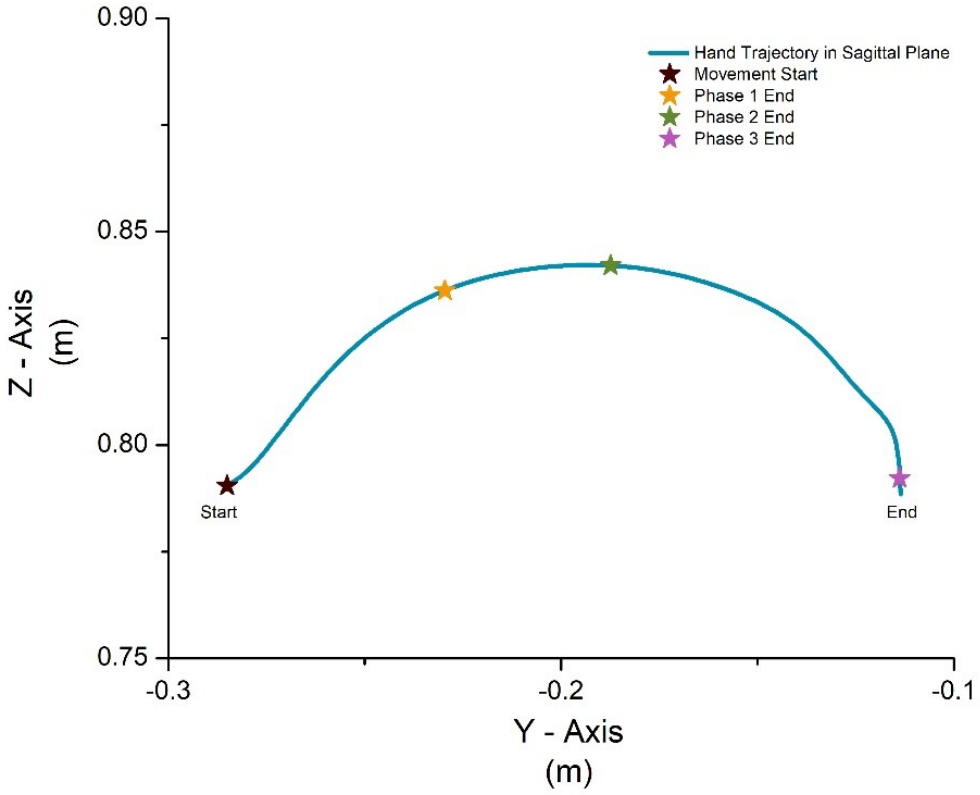

Figure 12: Hand Trajectory in Sagittal Plane

3.1.2 Joint Coordinate System and DOF Displacements

In the study, 7 DOF are prominently described for ease of data visualization and analysis. Figure 13 shows the phase-wise distribution of DOF excursions where the positive Y-axis denotes flexion and negative Y-axis denotes extension. The forward reaching movement was performed mainly through, shoulder flexion (30°) and elbow extension (40°) due to the biomechanical demand of the reaching movement. DOF other than shoulder flexion and elbow extension rotate due to the different trajectory configuration adopted by human arm.

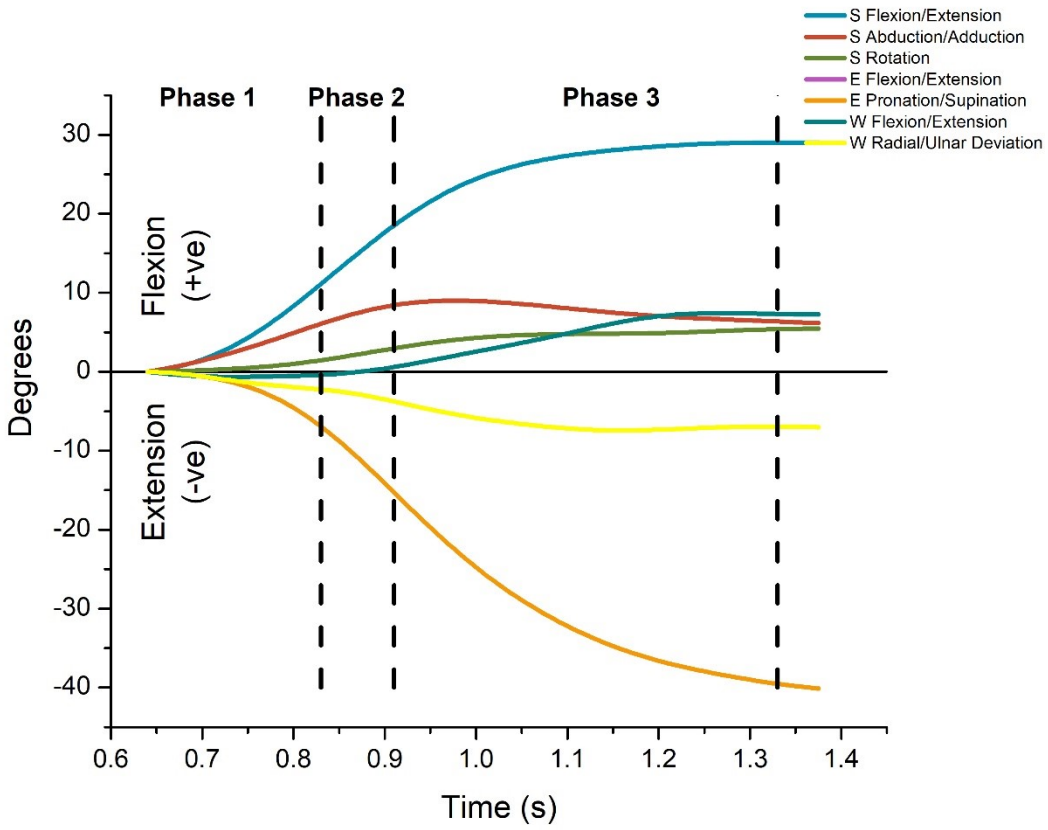

Figure 13: DOF Excursions

Table 4 below shows phase-wise breakdown of DOF displacement; the amount of rotation by one DOF during a phase. For forward reaching movement, shoulder gradually flexes till phase 2 while remains almost constant of around 30° during phase 3 on the other hand, elbow gradually increases with a peak of around -40° (negative sign indicates extension) in phase 3.

The basic DOF pattern followed for reaching is first the shoulder flexes and adjusts the elbow to the target then the elbow extends to rotate the object to the desired location.

Table 4: Phase-wise mean and standard deviation of amplitudes

DOF	Phase 1	Phase 2	Phase 3	Total
S. Flexion/Extension	11.6(3.16)	9.27(2.30)	10.3(3.43)	31.2(2.96)
S. Abduction/Adduction	6.51(3.03)	2.95(1.01)	-0.96(2.57)	8.51(2.20)
S. Rotation	1.20(0.42)	0.93(0.22)	1.52(0.87)	3.29(0.50)
E. Flexion/Extension	-7.32(2.54)	-11.2(2.59)	-23.0(6.33)	-41.6(3.82)
E. Pronation/Supination	-0.85(1.18)	-0.51(0.62)	0.83(0.86)	-0.54(0.88)
W. Flexion/Extension	-1.99(2.92)	0.20(0.67)	2.99(0.48)	1.20(1.35)
W. Radial/Ulnar Deviation	-0.63(4.27)	-1.90(1.24)	-2.12(2.45)	-4.60(2.65)

3.1.3 DOF Contribution to Hand Velocity

Figure 14shows the contribution of motion at each DOF to the hand velocity. From the figure, for phase 1, the major contributing DOF to the hand velocity is due to shoulder flexion. During phase 2 where shoulder flexion contribution starts decreasing, elbow extension DOF contribution to hand velocity increases resulting in the slight decrease in hand velocity. For phase 3, major contribution to hand velocity is due to the extension of elbow resulting in the elbow joint.

Table 5: DOF contribution to hand velocity

Phases	S. Flex/Ext	S. Ab/Ad	S. Rotation	E. Flex/Ext	E. Pro/Supi	W. Flex/Ext	W. Rad/Uln
Phase 1	0.25(0.03)	0.03(0.08)	0.00(0.00)	-0.01(0.01)	0.00(0.00)	0.00(0.00)	0.00(0.00)
Phase 2	0.25(0.03)	0.00(0.00)	0.00(0.00)	0.15(0.03)	0.00(0.00)	0.00(0.00)	0.00(0.00)
Phase 3	0.09(0.01)	0.00(0.00)	0.00(0.00)	0.17(0.02)	0.00(0.00)	0.00(0.00)	0.00(0.00)
Total Contr.	0.51(0.08)	0.03(0.01)	0.01(0.00)	0.31(0.07)	0.00(0.00)	0.00(0.00)	0.00(0.00)

3.1.4 Joint Control

The dynamics of the forward unloaded movement were calculated to determine the distribution of the torques at the joints throughout the movement. Torques at

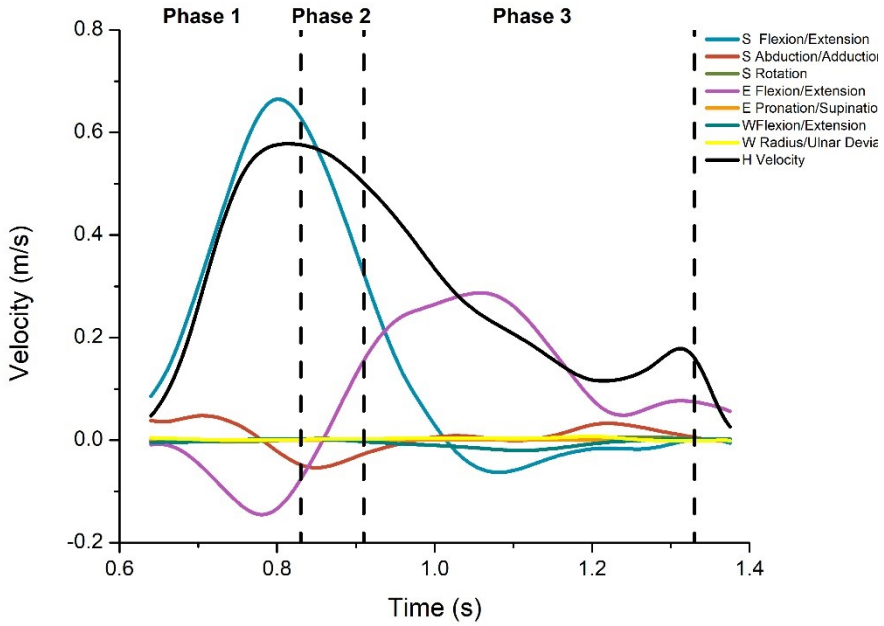

Figure 14: DOF Excursions

shoulder, elbow and wrist were calculated by Newton-Euler equations of motion across non-orthogonal effective axes described in the study by Hirashima et. al in 2006. NT obtained for this movement was in the range of 6.29E-04 – 2.68 Nm at the shoulder joint, between 3.51E-05 – 0.8 Nm at the elbow joint and 1.22E-06– 0.002 Nm at the wrist joint as shown in Figure 15. MT contribution (MTC) was computed as the ratio of signed MT projections on NT to the magnitude of NT at each joint. MTC values suggested the action of MT in rotating the joint. Values being close to 0 at a joint proposed that the joint was moving passively due to the sum of GT and IT, and values close to 1 indicated the joint to be moved actively, predominantly because of MT. Movement phases were defined at the time values where switching of control at the shoulder and elbow from active to passive and/or vice versa joints

were observed. Table 6 describes the mean phase characteristics obtained from all subjects where three phases were observed during forward reach.

Table 6: MTC for forward reaching

Joint	Phase 1	Phase 2	Phase 3
Shoulder	0.99(0.12)	0.04(0.07)	0.00(0.11)
Elbow	0.00(0.13)	0.00(0.12)	0.98(0.11)
Wrist	0.78(0.12)	0.67(0.14)	0.34(0.10)
Active Joint	Shoulder	Both Passive	Elbow

Phase-wise separation of the torques shows the leading joint bias (Figure 15). For phase 1, shoulder NET is assisted with the positive muscle torque while elbow NT acts passively due to GT and IT. The control shifts for phase 2 where elbow NT is assisted by the muscle torques and shoulder joint moves passively. Analysis of wrist movement suggests that MT mainly compensates for passive torques and provides adjustments of the wrist motion according to the requirement of the task.

3.2 Shoulder Level Reaching Movement

3.2.1 Hand Trajectory in Sagittal Plane

Similar to the hand trajectory displayed in forward reaching movement, hand trajectory across the sagittal plane i.e. Y-Z plane is shown in figure 16. Here, larger displacement across vertical plane is observed. The horizontal displacement along Y- axis of the hand is about 0.2 m and the vertical displacement along Z – axis of the hand is about 0.3 m. An additional phase can be in this movement.

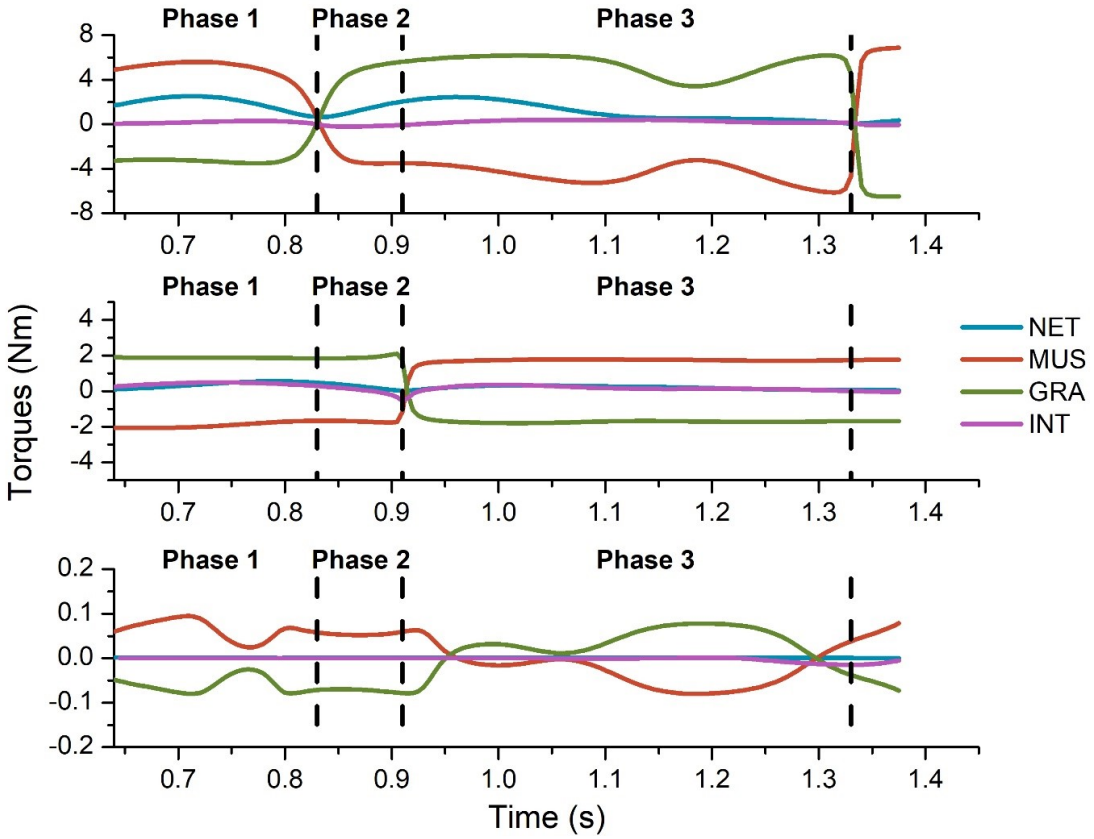

Figure 15: Torque Projections for Forward Reaching Movement

3.2.2 Joint Coordinate System and DOF Displacements

Similar to the DOF displacement graph for forward reaching movement, Figure 17 shows the DOF excursions for shoulder reach movement. The upward reaching movement as forward reaching movement was performed mainly through, shoulder flexion (50°) but in this movement elbow first undergoes flexion of about (10°) and then extension (35°) due to the biomechanical demand of the reaching movement. In this movement, elbow undergoes flexion to provide enough space for the arm to rotate the soda can to the shoulder height. DOF other than shoulder flexion and

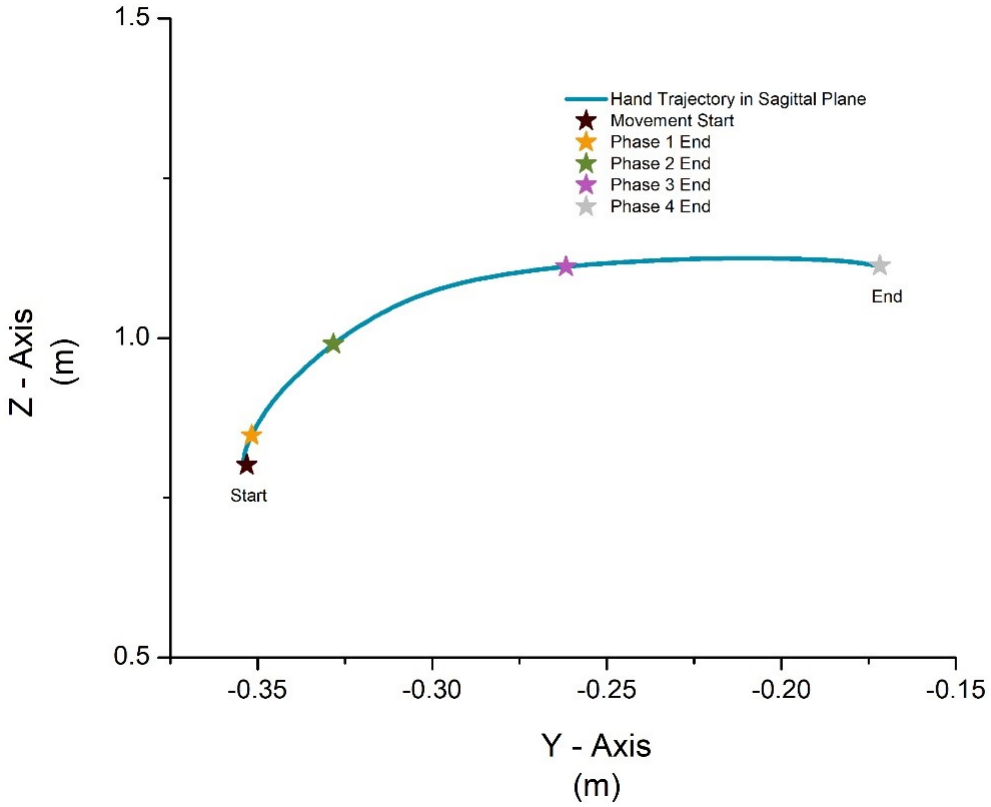

Figure 16: Hand Trajectory in Sagittal Plane

elbow flexion/extension rotate due to the different trajectory configuration adopted by human arm.

Table 7 shows phase-wise breakdown of DOF displacement; the amount of rotation by one DOF during a phase. For shoulder reaching movement, shoulder gradually flexes till end phase while remains almost constant of around 50° at the end of phase 4 on the other hand, elbow first flexes at around 10° till phase 2 and then gradually extends with a peak of around -35° in phase 3 and phase 4.

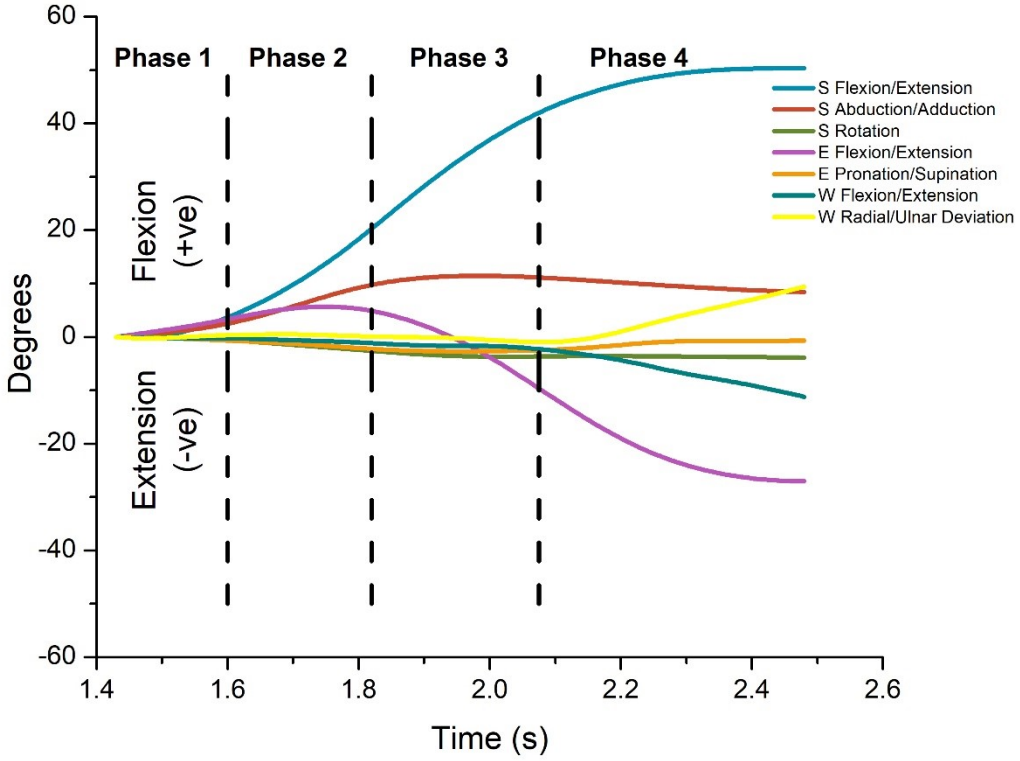

Figure 17: DOF Excursions for Shoulder Level Reaching Task

Table 7: Phase-wise mean and standard deviation of DOF amplitudes

DOF	Phase 1	Phase 2	Phase 3	Phase 4	Total
S. Flexion/Extension	2.71(0.65)	17.2(1.98)	21.1(1.98)	10.2(1.93)	54.3(1.39)
S. Abduction/Adduction	1.88(0.57)	6.21(0.65)	1.87(1.23)	-4.15(0.65)	5.82(0.77)
S. Rotation	-0.12(0.11)	-0.60(0.12)	-0.18(0.17)	0.22(0.17)	-0.69(0.20)
E. Flexion/Extension	2.07(0.33)	0.14(0.33)	-17.4(0.74)	-23.5(1.44)	-38.7(1.01)
E. Pronation/Supination	-1.07(0.23)	-1.46(0.40)	-0.82(0.19)	1.08(0.30)	-2.27(0.28)
W. Flexion/Extension	-1.32(0.24)	-3.57(1.05)	-1.89(0.68)	-1.60(0.53)	-8.38(0.63)
W. Radial/Ulnar Deviation	-0.09(0.64)	-0.56(1.25)	-0.58(0.82)	1.22(0.81)	-0.01(0.88)

3.2.3 DOF Contribution to Hand Velocity

Figure 18 shows the contribution of motion at each DOF to the hand velocity for shoulder reaching movement. From the Figure 18, for phase 1, the major contribut-

ing DOF to the hand velocity is due to shoulder and elbow flexion. During phase 2 where shoulder flexion contribution is still increasing, elbow flexion switches to extension and DOF contribution to hand velocity solely is due to shoulder flexion. This DOF contribution by shoulder flexion decreases in phase 3 while elbow DOF contribution by elbow increases. It is interesting that when the DOF contribution bias switches from shoulder to elbow, the arm is moving passively. Finally, in phase 4 is solely because of elbow extension.

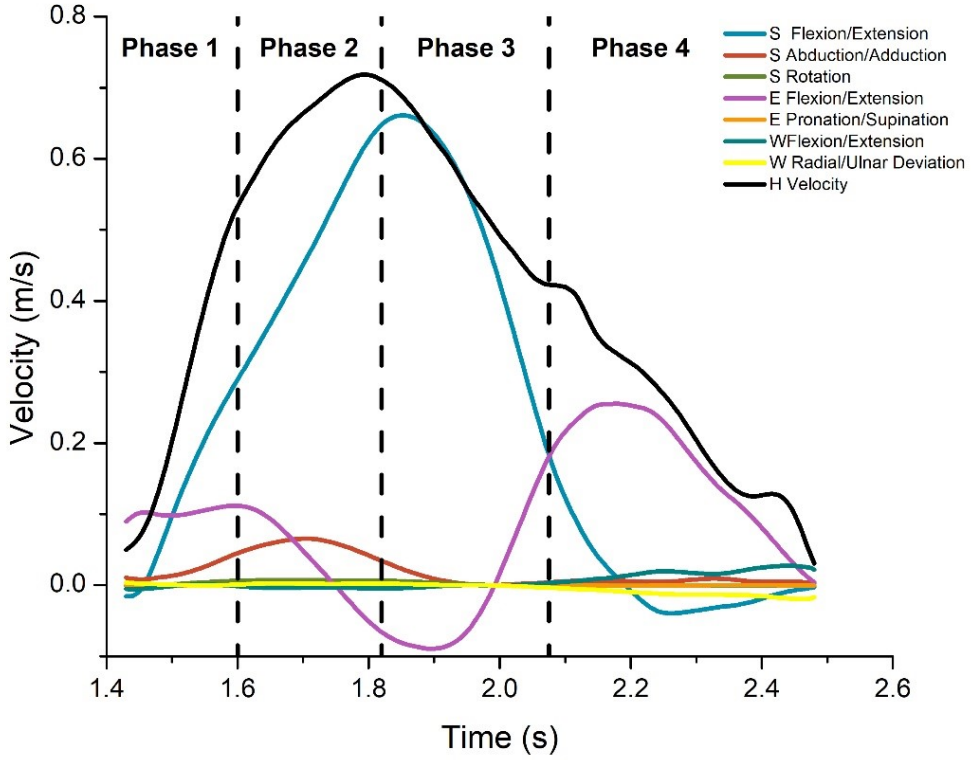

Figure 18: DOF contribution to Hand Velocity for Shoulder Level Reaching Task

Figure 19 shows the contribution of motion at each DOF to the hand velocity

Table 8: DOF contribution to Hand Velocity for Shoulder Level Reaching Task

Phases	S.Flex/Ext	S.Ab/Ad	S.Rotation	E.Flex/Ext	E.Pro/Supi	W.Flex/Ext	W.Rad/Uln
Phase 1	0.13(0.05)	0.02(0.01)	0.00(0.00)	0.08(0.03)	0.00(0.00)	0.00(0.00)	0.00(0.00)
Phase 2	0.56(0.05)	0.03(0.01)	0.00(0.00)	0.02(0.02)	0.00(0.00)	-0.01(0.00)	0.00(0.00)
Phase 3	0.56(0.06)	0.01(0.00)	0.00(0.00)	0.01(0.03)	0.00(0.00)	0.00(0.00)	0.00(0.00)
Phase 4	0.01(0.03)	0.01(0.01)	0.00(0.00)	0.21(0.05)	0.00(0.00)	0.00(0.00)	0.00(0.00)
Total Cont.	1.26(0.20)	0.09(0.04)	0.00(0.00)	0.34(0.14)	0.00(0.01)	-0.02(0.01)	0.00(0.00)

for shoulder reaching movement. From the figure, for phase 1, the major contributing DOF to the hand velocity is due to shoulder and elbow flexion. During phase 2 where shoulder flexion contribution is still increasing, elbow flexion switches to extension and DOF contribution to hand velocity solely is due to shoulder flexion. This DOF contribution by shoulder flexion decreases in phase 3 while elbow DOF contribution by elbow increases. It is interesting that when the DOF contribution bias switches from shoulder to elbow, the arm is moving passively. Finally, in phase 4 is solely because of elbow extension.

3.2.4 Joint Control

The NT torque obtained for this movement was in the range of 2 - 4 Nm at the shoulder joint, between 0.006 – 0.4 Nm at the elbow joint and 2.31E-04 – 0.009 Nm at the wrist joint as shown in Figure 19. Table 9 describes the mean phase characteristics observed by the data set where four phases were observed during shoulder reach.

Phase-wise separation of the torques shows the leading joint bias (Figure 19). For phase 1, both shoulder and elbow NT are supported by positive MT. The elbow control shifts for phase 2 where elbow NT is supported passively by GT and IT and shoulder joint moves due to the aid of MT. During phase 3, both joints moves pas-

Table 9: MTC for shoulder level reaching

Joint	Phase 1	Phase 2	Phase 3	Phase 4
Shoulder	0.99(0.00)	0.99(0.00)	0.02(0.11)	0.00(0.00)
Elbow	0.99(0.00)	0.00(0.00)	0.00(0.11)	0.98(0.00)
Wrist	0.41(0.12)	0.47(0.10)	0.73(0.10)	0.38(0.06)
Active Joint	Both Active	Shoulder	Both Passive	Elbow

sively, this may be due to the switching of joint control for both joints simultaneously. Lastly, during phase 4, elbow extension leads the joint control solely. Again, analysis of wrist movement suggests that MT mainly compensates for passive torques and provides adjustments of the wrist motion according to the requirement of the task.

3.3 Eye Level Reaching Movement

3.3.1 Hand Trajectory in Sagittal Plane

Again, a similar pattern of hand trajectory to that of upward shoulder is observed in eye reaching movement. The horizontal displacement in this movement is 0.2 m along Y – axis while the vertical displacement is about 0.5 m.

3.3.2 Joint Coordinate System and DOF Displacements

Similar to the DOF displacement graph for shoulder reaching movement, Figure 21 shows the DOF excursions for eye reach movement. The eye reaching movement follows a similar pattern for DOF rotation as that of shoulder reaching with shoulder

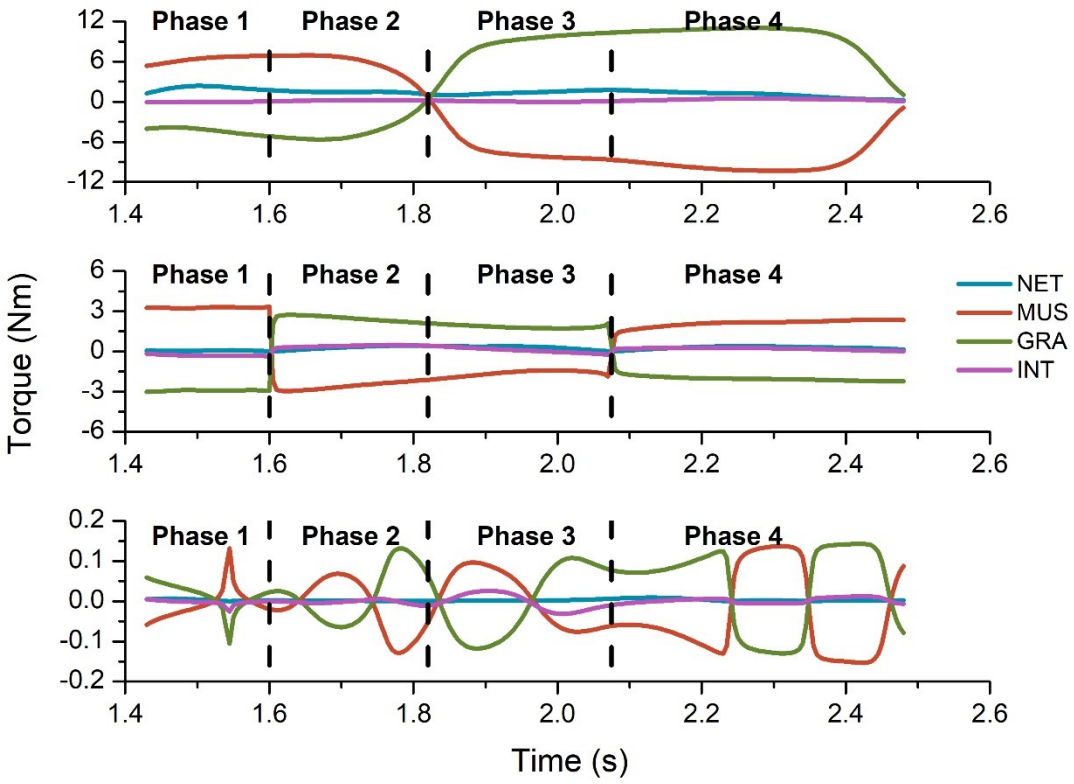

Figure 19: Torque Projections for Shoulder Level Reaching Movement

flexion (80°) but in this movement elbow first undergoes flexion of about (10°) and then extension (40°) due to the biomechanical demand of the reaching movement.

Table 10 shows phase-wise breakdown of DOF displacement; the amount of rotation by one DOF during a phase. For eye reaching movement, shoulder gradually flexes till end phase while remains almost constant of around 68° at the end of phase 4 on the other hand, elbow first flexes at around 10° till phase 2 and then gradually extends with a peak of around -50° in phase 3 and phase 4.

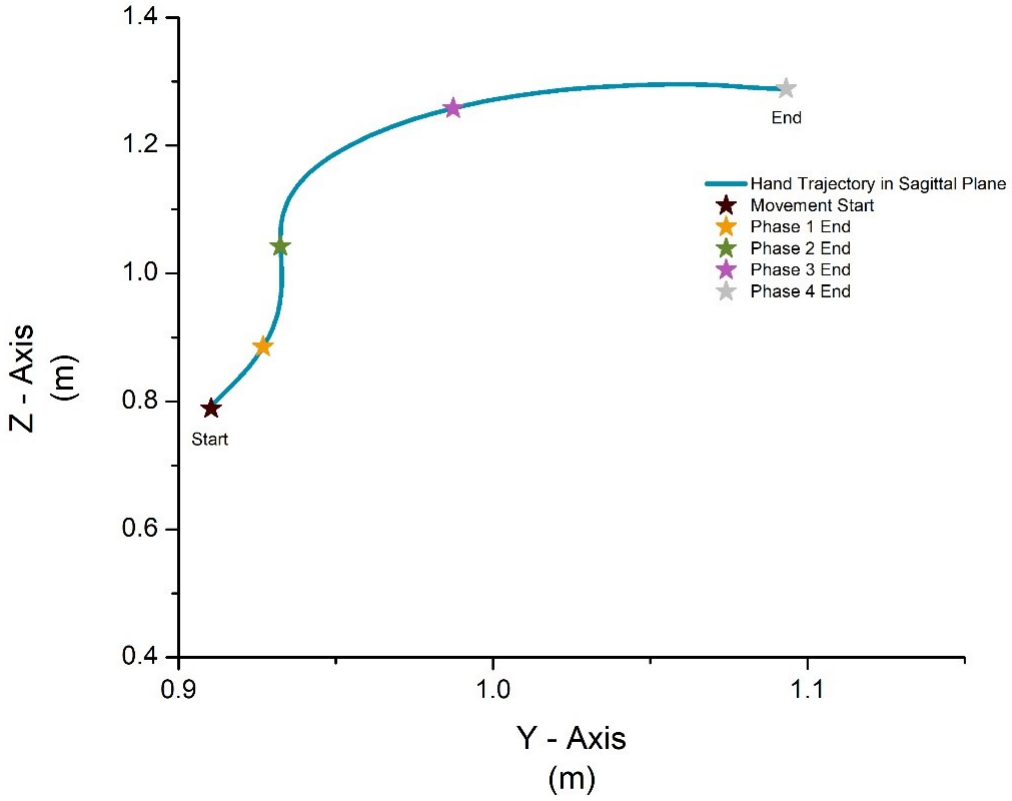

Figure 20: Hand Trajectory in Sagittal Plane for Eye Level Task

Table 10: Phase-wise mean and standard deviation of DOF amplitudes

DOF	Phase 1	Phase 2	Phase 3	Phase 4	Total
S. Flexion/Extension	3.76(0.70)	21.3(2.94)	31.5(2.78)	12.3(1.38)	58.9(1.95)
S. Abduction/Adduction	2.90(0.59)	8.81(1.05)	2.08(0.75)	-6.67(1.49)	7.13(0.97)
S. Rotation	-0.26(0.17)	-1.86(0.23)	-1.32(0.27)	0.14(0.25)	-3.31(0.23)
E. Flexion/Extension	3.57(0.79)	2.06(0.70)	-25.3(1.91)	-30.4(1.62)	-50.1(1.25)
E. Pronation/Supination	-1.21(0.36)	-2.05(0.65)	-1.22(0.63)	1.83(0.44)	-2.65(0.52)
W. Flexion/Extension	-1.82(0.60)	-4.43(0.48)	-2.62(1.15)	-3.11(0.52)	-11.9(0.69)
W. Radial/Ulnar Deviation	0.05(1.29)	0.31(1.77)	-0.36(0.55)	3.41(1.47)	-3.43(1.25)

3.3.3 DOF Contribution to Hand Velocity

Figure 22 shows the contribution of motion at each DOF to the hand velocity for eye reaching movement. The DOF contribution to hand velocity is similar to that of

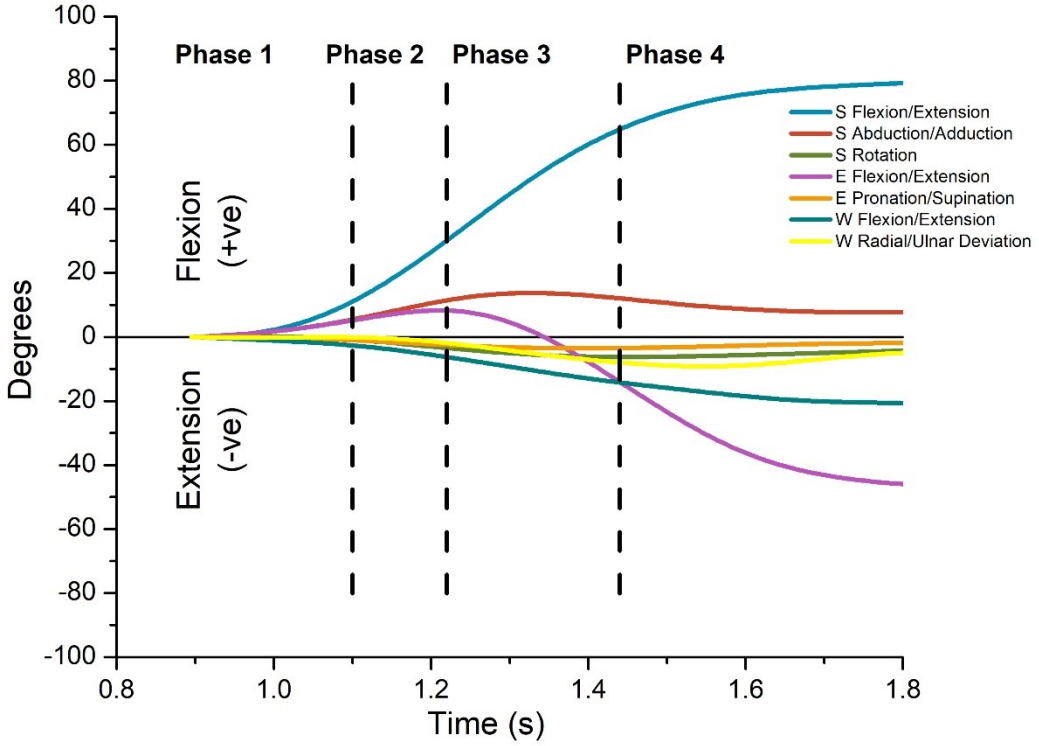

Figure 21: DOF Excursions for Eye Level Task

shoulder reaching movement where for phase 1 and about half of phase 2, majority of contributors are shoulder and elbow flexion. During phase 3, DOF contribution to hand velocity is due to the decreasing of the velocity of shoulder flexion and increasing in the velocity at which elbow extends.

Table 11: DOF contribution to Hand Velocity for Eye Level Reaching Task

Phases	S.Flex/Ext	S.Ab/Ad	S.Rotation	E.Flex/Ext	E.Pro/Supi	W.Flex/Ext	W.Rad/Uln
Phase 1	0.16(0.06)	0.05(0.03)	0.00(0.00)	0.16(0.07)	-0.01(0.01)	-0.04(0.04)	0.08(0.08)
Phase 2	0.88(0.32)	0.26(0.21)	0.01(0.02)	0.13(0.09)	-0.02(0.02)	-0.10(0.09)	0.32(0.02)
Phase 3	1.44(0.82)	0.23(0.21)	-0.07(0.07)	-0.49(0.53)	-0.09(0.09)	-0.07(0.06)	0.42(0.04)
Phase 4	0.20(0.25)	-0.10(0.15)	0.03(0.03)	-0.23(0.52)	0.00(0.00)	-0.18(0.10)	0.05(0.05)
Total Cont.	2.70(1.45)	0.45(0.62)	-0.05(0.14)	-0.43(1.22)	-0.14(0.14)	-0.41(0.30)	0.21(0.20)

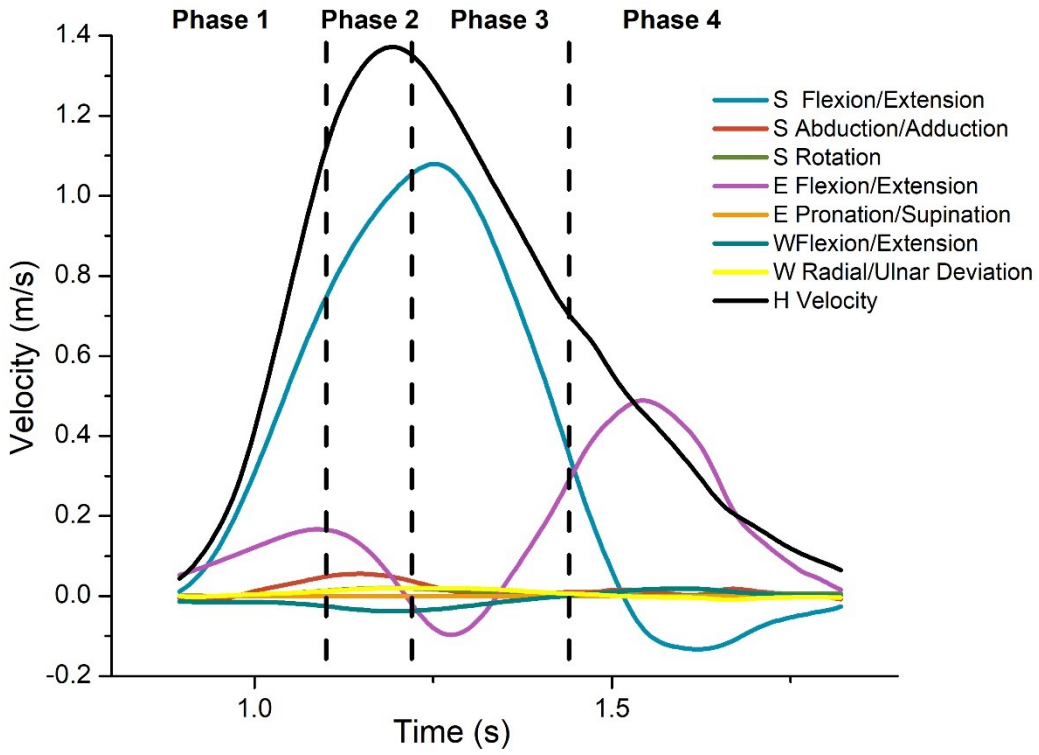

Figure 22: DOF contribution to Hand Velocity for Eye Level Reaching Task

It can be seen from table 12 like shoulder reaching movement, for phase 1, majority of the contribution to the hand velocity is due to the combination of shoulder and elbow flexion about (0.16 m/s for shoulder flexion and 0.16 m/s for elbow flexion). In phase 2, shoulder takes over the contribution to hand velocity while elbow flexion contribution decreases. In phase 3, shoulder is still contribution to the hand velocity while elbow switches from elbow flexion to extension. And in phase 4, elbow extension solely contributes to the hand velocity (-0.23 m/s).

3.3.4 Joint Control

The NT torque obtained for this movement was in the range of 0.33 - 4 Nm at the shoulder joint, between 0.008 – 1.03 Nm at the elbow joint and 1.23E-04 – 0.0076 Nm at the wrist joint as shown in Figure 23. Table 12 describes the typical phase characteristics observed by the data set where four phases were observed during shoulder reach.

Table 12: MTC for Eye Level Reaching

Joint	Phase 1	Phase 2	Phase 3	Phase 4
Shoulder	1.00(0.00)	0.92(0.00)	0.01(0.00)	0.07(0.00)
Elbow	0.94(0.06)	0.06(0.01)	0.02(0.03)	0.96(0.01)
Wrist	0.41(0.13)	0.48(0.07)	0.56(0.12)	0.36(0.09)
Active Joint	Both Active	Shoulder	Both Passive	Elbow

Phase-wise separation of the torques shows the leading joint bias (Figure 23). For phase 1, both shoulder and elbow NT are supported by positive MT. The elbow control shifts for phase 2 where elbow NT is supported passively by GT and IT and shoulder joint moves due to the aid of MT. During phase 3, both joints moves passively, this may be due to the switching of joint control for both joints simultaneously. Lastly, during phase 4, elbow extension leads the joint control solely. This movement is like that of shoulder reaching.

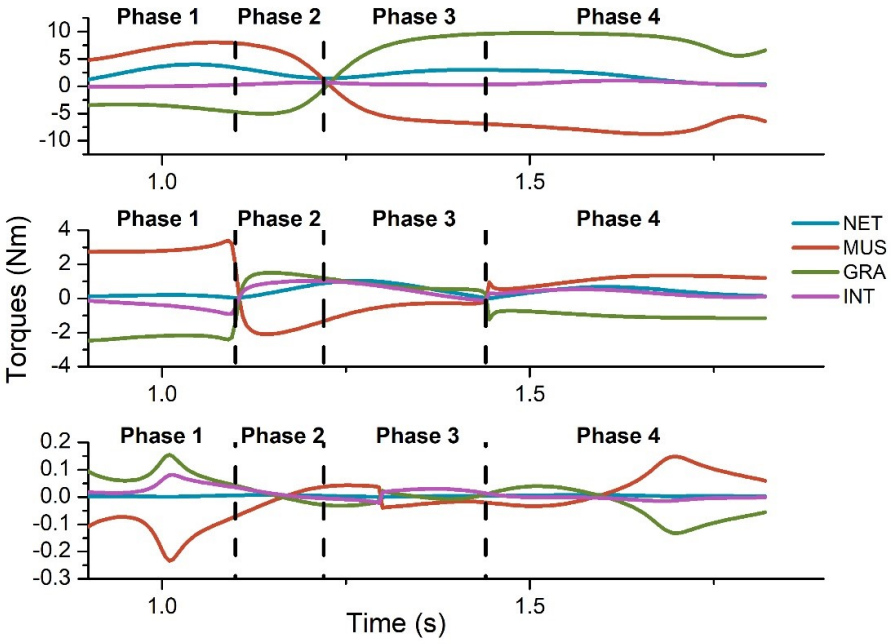

Figure 23: Torque Projections for Eye Level Reaching Movement

3.4 Additional Phases

Additional phases were observed for less than 5% of the total time period. The probability of the occurrence of these phases was 80% for forward reaching, 68% for shoulder level reaching and 37% for eye level reaching. These phases observed, may be the result of static holding of the empty soda can at the final position. One example of the presence of additional phase can be seen in the Figure 24 below

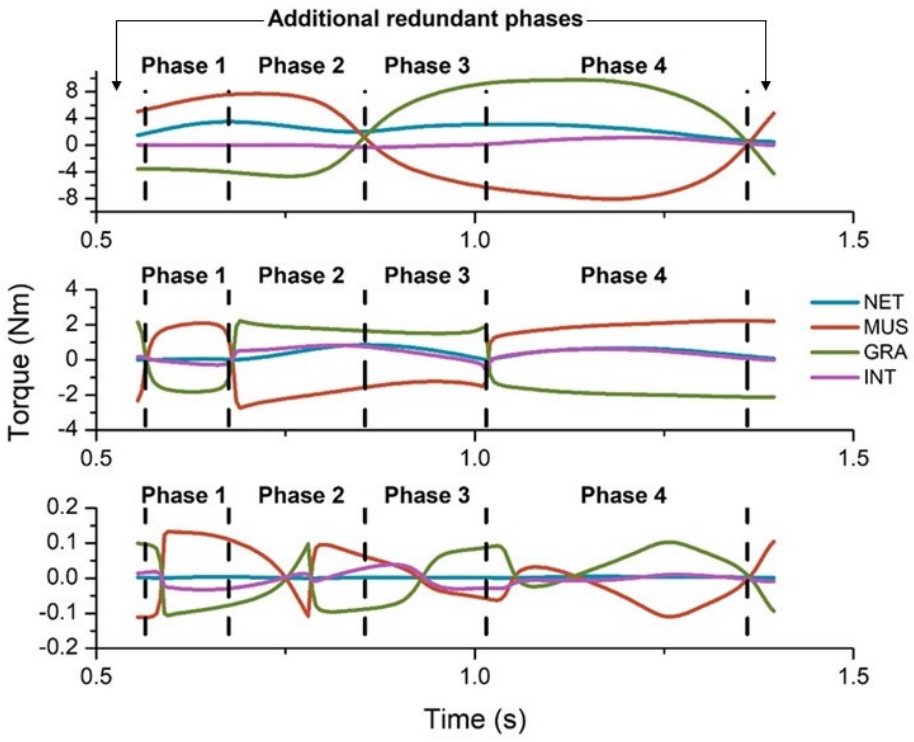

Figure 24: Additional Observed Phases

Chapter 4

CONCLUSION

The chief conclusions derived are as follows:

4.1 Common Traits (Patterns similar to all three reaching movements)

• Other than the vertical Z – axis displacement in the sagittal plane, the trajectory of hand in sagittal plane suggests the point-to-point smooth transition in all three-reaching movements. The smooth trajectory shows optimum pathway adopted by the hand in the phase transition. Analysis of this factor may provide further insight in the cost function (optimum control theory) in the position and trajectory control of movement.

• DOF rotation amplitudes shows averaged values for rotation of DOF for this movement. The displacements show the prevalence of the rotation of shoulder flexion and elbow extension DOF.

• Contribution of each DOF in the hand velocity, shows the high contribution of the shoulder flexion and elbow extension to the total hand velocity in reaching movements.

• Wrist control is observed to be stable for most of the movement due to the compensation of MT to PT throughout the trail period for all three movements.

4.2 Forward Reaching

• Prevalence of leading joint was observed for shoulder in the Phase 1 of the movement suggesting the rotation of shoulder DOF (Flexion/Extension). This demonstrated that the MT at shoulder joint supported the rotation while PT provided the mechanical interaction to rotate the elbow and wrist joint. The rotation of shoulder in phase 1 adjusts the trajectory to provide an optimum path to final position.

• During phase 2, both joints were observed to be passive, suggesting the rotation of joints solely due to the PT. In this phase, the anatomical DOF may be in a state of equilibrium enabling the switching the control of torques.

• In phase 3, elbow DOF (Extension) takes precedence in the control of joint rotation while, shoulder rotates passively. Here, shoulder remains passive while the MT at elbow rotates the elbow DOF to the final position.

• The additional phases accounted for in some trials, might be due the static holding of the soda can have placed at the final position. At this position, due to the holding phase, MT at shoulder and elbow are in a state of equilibrium explaining the MTC values in this phase to be 1.

4.3 Shoulder Level Reaching

• In phase 0, MTC value for both joints, shoulder and elbow are close to 1. At the start of the movement, both joints move in an active state suggesting rotation of both joints simultaneously that is, MT contributes in the rotation at both joints. This

is an interesting change as this can be due to the change in the synergies adopted by the arm or due to the employment of different muscles in the rotation of the same joint i.e., DOF redundancy.

• From phase 1 the controls exhibited by the arm are similar to that observed in forward reaching which starts with the leading joint being shoulder, while elbow trails. Both shoulder and elbow remain passive during the phase 2 which might suggest a position of equilibrium of joint. Finally, in Phase 3, elbow takes over the control while shoulder moves passively.

• Additional phases observed at the end of the trial like in forward reaching may indicate the equilibrium of both shoulder and elbow joints to maintain the static hold position.

• As in forward reaching, wrist control is observed to be stable due to the compensation of MT to PT throughout the movement.

4.4 Eye Level Reaching

• The control observed in this movement closely matches the control observed in shoulder-reaching movement. kinematics and kinetics pattern observed in this movement are similar to that in shoulder-level reaching tasks.

4.5 Implications in Biomedical Application

LJH provides a simple, flexible analysis which can be applied to both single and multi-joint movements. Using the kinematic and kinetic results, not only rehabilitation robots can be developed with the parameters to compensate for the lack in

MT and improve IT profile but also design robots which imitate reaching movement based on the above study. LJH concept can be also translated to the optimization of joint movement in athletes, by focusing on the MT contribution in a particular athletic movement. This can help an athlete to follow an efficient workout and improve his/her performance. Despite LJH's merits, different strategies employed by the same joints in the same movement are not supported by this hypothesis. Combining this hypothesis with other theories may provide better insights into understanding control patterns of the multi-joint segment.

REFERENCES

Ahmed, et al., Alaa A. 2008. "Flexible Representations of Dynamics Are Used in Object Manipulation." *Current Biology* 18 (10): 763–768.

Artemiadis, Panagiotis. 2013. "Closed-Form Inverse Kinematic Solution for Anthropomorphic Motion in Redundant Robot Arms." *Advances in Robotics & Automation* 2 (3).

Asada, Harry. 2005. "Introduction to Robotics - MIT Open Courseware." https://ocw.mit.edu/courses/mechanical-engineering/2-12-introduction-to-robotics-fall-2005/lecture-notes/.

Asmussen, et al., Michael J. 2014. "Intersegmental Dynamics Shape Joint Coordination during Catching in Typically Developing Children but Not in Children with Developmental Coordination Disorder."" *Journal of Neurophysiology* 111 (7): 1417–1428.

Caillou, et al., N. 2002. "Overcoming Spontaneous Patterns of Coordination during the Acquisition of a Complex Balancing Task." *Canadian Journal of Experimental Psychology/Revue Canadienne De Psychologie ExpÃ©Rimentale* 56 (4): 283–293.

Craig, John J. 2004. *Introduction to Robotics: Mechanics and Control*. Third. Pearson.

Debicki, et al., Derek B. 2010. "Wrist Muscle Activation, Interaction Torque and Mechanical Properties in Unskilled Throws of Different Speeds." *Experimental Brain Research* 208 (1): 115–125.

Dounskaia, & Goble J. A., N. 2011a. "The role of vision, speed, and attention in overcoming directional biases during arm movements." *Experimental Brain Research* 209 (2): 299–309.

Dounskaia, & Shimansky Y., N. 2016. "Strategy of arm movement control is determined by minimization of neural effort for joint coordination." *Experimental Brain Research* 234 (6): 1335–1350.

Dounskaia, & Wang W., N. 2014a. "A preferred pattern of joint coordination during arm movements with redundant degrees of freedom." *Journal of Neurophysiology* 112 (5): 1040–53.

Dounskaia, et al., N. 2002. "Commonalities and Differences in Control of Various Drawing Movements." *Experimental Brain Research* 146 (1): 11–25.

Dounskaia, Goble J. A. & Wang W., N. 2011b. "The role of intrinsic factors in control of arm movement direction: implications from directional preferences." *Journal of Neurophysiology* 105 (3): 999–1010.

Dounskaia, Natalia. 2010. "Control of Human Limb Movements: The Leading Joint Hypothesis and Its Practical Applications." *Exercise and Sport Sciences Reviews* 38 (4): 201–208.

Dounskaia, Natalia, and Wanyue Wang. 2014. "A Preferred Pattern of Joint Coordination during Arm Movements with Redundant Degrees of Freedom." *Journal of Neurophysiology* 112 (5): 1040–1053.

Dounskaia, Wang W. Sainburg R. L. & Przybyla A., N. 2014b. "Preferred directions of arm movements are independent of visual perception of spatial directions." *Experimental Brain Research* 232 (2): 575–586.

Feldman, A.g., and M. Ghafouri. 2001. "he Timing of Control Signals Underlying Fast Point-to-Point Arm Movements." *Experimental Brain Research* 137 (3-4): 411–423.

Feldman, Anatol G. 1986. "Once More on the Equilibrium-Point Hypothesis (Î» Model) for Motor Control." *Journal of Motor Behavior* 18 (1): 17–54.

Feltner, Michael E., and September T. Nelson. 1996. "Three-Dimensional Kinematics of the Throwing Arm during the Penalty Throw in Water Polo." *Journal of Applied Biomechanics* 12 (3): 359–382.

Franklin, David W., and Daniel M. Wolpert. 2011. "Computational Mechanisms of Sensorimotor Control." *Neuron* 72 (3): 425–442.

Gillard, Yakovenko S. Cameron T. & Prochazka A., D. M. 2000. "Isometric muscle length–tension curves do not predict angle–torque curves of human wrist in continuous active movements." *Journal of Biomechanics* 33 (11): 1341–1348.

Goble, Zhang Y. Shimansky Y. Sharma S. & Dounskaia N. V., J. A. 2007. "Directional Biases Reveal Utilization of Arm's Biomechanical Properties for Optimization of Motor Behavior." *Journal of Neurophysiology* 98 (3): 1240–1252.

Hartley, R. V. L. 1928. "Transmission of Information." *1. Bell System Technical Journal* 7 (3): 535–563.

Hirashima, & Ohtsuki T., M. 2008a. "Exploring the Mechanism of Skilled Overarm Throwing." *Exercise and Sport Sciences Reviews* 36 (4): 205–211.

Hirashima, et. al., Masaya. 2007. "A New Non-Orthogonal Decomposition Method to Determine Effective Torques for Three-Dimensional Joint Rotation (Supplementary Text)." *Journal of Biomechanics* 40 (4): 871–882.

Hirashima, et al, Masaya. 2008b. "Kinetic Chain of Overarm Throwing in Terms of Joint Rotations Revealed by Induced Acceleration Analysis." *Journal of Biomechanics* 41 (13): 2874–2883.

Hirashima, et al., Masaya. 2003a. "Utilization and Compensation of Interaction Torques During Ball-Throwing Movements." *Journal of Neurophysiology* 89 (4): 1784–1796.

Hirashima, et al, Masaya. 2003b. "Utilization and Compensation of Interaction Torques During Ball-Throwing Movements." *Journal of Neurophysiology* 89 (4): 1784–1796.

Hirashima, Masaya, and Daichi Nozaki. 2012. "Distinct Motor Plans Form and Retrieve Distinct Motor Memories for Physically Identical Movements." *Current Biology* 22 (5): 432–436.

Hirashima, Ohgane K. Kudo K. Hase K. & Ohtsuki T., M. 2003c. "Counteractive Relationship Between the Interaction Torque and Muscle Torque at the Wrist Is Predestined in Ball-Throwing." *Journal of Neurophysiology,* 90 (3): 1449–1463.

Latash, Mark L. 2010. "Motor Synergies and the Equilibrium-Point Hypothesis." *Motor Control* 14 (3): 294–322.

Leva, P de. 1996. "Adjustments to Zatsiorsky-Seluyanov's segment inertia parameters." *Journal of Biomechanics* 29 (9): 1223–1230.

Loeb, Brown I. E. & Cheng E. J., G. E. 1999. "A hierarchical foundation for models of sensorimotor control." *Experimental Brain Research* 126 (1): 1–18.

Mihelj, Matjaž. 2006. "Inverse Kinematics of Human Arm Based on Multisensor Data Integration." *Journal of Intelligent and Robotic Systems* 47 (2): 139–153.

NA., Bernstein. 1967. "The Co-ordination and Regulation of Movements." *Pergamon Press; Oxford:*

NA, Bernstein. 1935. "The problem of interrelation between coordination and localization." *Archives of Biological Science. (in Russian)* 38:1–35.

Oldfield, R. C. 1971. "The assessment and analysis of handedness." *The Edinburgh inventory. Neuropsychologia* 9 (1): 97–113.

Otten, E. 2005a. "Multi-Joint Dynamics and the Development of Movement Control." *Neural Plasticity* 12 (2-3): 89–98.

Otten, E. 2005b. "Multi-Joint Dynamics and the Development of Movement Control." *Neural Plasticity* 12 (2-3): 89–98.

Papi, et al., Enrica. 2015. "Analysis of Gait within the Uncontrolled Manifold Hypothesis: Stabilisation of the Centre of Mass during Gait." *Journal of Biomechanics* 48 (2): 324–331.

Scholz, & et. al. 2014. "Use of the Uncontrolled Manifold (UCM) Approach to Understand Motor Variability, Motor Equivalence, and Self-Motion." *Advances in Experimental Medicine and Biology Progress in Motor Control:* 91–100.

Schütz, & Schack T., C. 2013. "Motor primitives of pointing movements in a three-dimensional workspace." *Experimental Brain Research* 227 (3): 355–365.

Shannon, C. E. 1948. "A Mathematical Theory of Communication." *Bell System Technical Journal* 27 (3): 379–423.

St-Onge, et al., N. 1997. "Control Processes Underlying Elbow Flexion Movements May Be Independent of Kinematic and Electromyographic Patterns: Experimental Study and Modelling." *Neuroscience* 79 (1): 295–316.

Vereijken, et al., B. 1997. "Changing Coordinative Structures in Complex Skill Acquisition." *Human Movement Science* 16 (6): 823–844.

Wang, & Dounskaia N, W. 2016. "Neural control of arm movements reveals a tendency to use gravity to simplify joint coordination rather than to decrease muscle effort." *Neuroscience* 339 (418–432).

Wang, N., W. & Dounskaia. 2015. "Influence of workspace constraints on directional preferences of 3D arm movements." *Experimental Brain Research* 233 (7): 2141–2153.

Wang, W. et. al. 2012. "Load emphasizes muscle effort minimization during selection of arm movement direction." *Journal of NeuroEngineering and Rehabilitation,* 9 (1): 70.

Wulf, & Schmidt R. A., G. 1989. "The learning of generalized motor programs: Reducing the relative frequency of knowledge of results enhances memory." *Journal of Experimental Psychology: Learning, Memory, and Cognition* 15 (4): 748–757.